C.P.No.559

C.P.No.559

MINISTRY OF AVIATION

AERONAUTICAL RESEARCH COUNCIL

CURRENT PAPERS

A Preliminary Study of Ionic Recombination of Argon in Wind Tunnel Nozzles

By

K. N. C. Bray and J. A. Wilson

LONDON: HER MAJESTY'S STATIONERY OFFICE
1961

SIX SHILLINGS NET

C.P. No.559

February, 1960

A Preliminary Study of Ionic Recombination of Argon in Wind Tunnel Nozzles

- By -

K. N. C. Bray and J. A. Wilson,
University of Southampton

The research reported in this document has been sponsored in part by the Wright Air Development Division of the Air Research and Development Command, United States Air Force, through its European Office

---

LIST OF CONTENTS

		Page
	Summary	2
	List of Symbols	2
1.	Introduction	3
2.	The Ideal Monatomic Gas in Equilibrium	4
3.	Discussion of the Rate Equation	8
4.	Quasi-One-Dimensional Flow Equations	11
5.	Non-Equilibrium Flow	15
6.	Conclusions	19
	Acknowledgments	20
	References	20

SUMMARY/

Previously issued as U.S.A.A. Report No.134 - A.R.C.22,326.

SUMMARY

The theory of the ideal ionising monatomic gas is briefly outlined and a Mollier chart is presented for this gas in equilibrium. Its flow through nearly conical nozzles is considered for cases where ionic recombination is either in complete equilibrium or completely frozen. A discussion is included of conditions under which the ionisation fraction becomes vanishingly small, when the gas behaves as a perfect gas.

A useable rate equation has not been developed for partial equilibrium calculations, but a method of attempting this problem has been suggested for the case of argon. In the absence of a suitable rate equation the quasi-one-dimensional flow equations have not been integrated for partial equilibrium cases, but criteria are given for the flow to be near to equilibrium and nearly frozen. If the assumptions made here are correct then these criteria suggest that there may be a lack of ionic equilibrium in the nozzles of plasma-jet wind tunnels when operated at low stagnation pressures. Departure from adiabatic flow due to photon emission is also considered, and shown to be negligible.

List of Symbols

A	area ratio	(dimensionless)
A'	area of nozzle at a given station	(ft^2)
A^*	area of nozzle at sonic throat	(ft^2)
c'	frozen velocity of sound	(ft/sec)
C_p	specific heat at constant pressure	($slugs^2/ft^4\,sec^2$)
C_v	specific heat at constant volume	($slugs/ft^4\,sec^2$)
e'	specific internal energy	(ft lb/slugs)
e'_r	radiated energy	(ft lb/slugs)
h	Plank's constant = 4.868×10^{-34}	(ft lb sec)
i'	specific enthalpy	(ft lb/slugs)
k	Boltzmann's constant = 1.019×10^{-23}	(ft lb/°K mol)
M	Mach number	(dimensionless)
M_c	frozen Mach number	(dimensionless)
m	mass of an atom	(slugs)
m_e	mass of an electron	(slugs)
m_+	mass of an ion	(slugs)
n'	overall number density	(ft^{-3})
n'_a	number density of atoms	(ft^{-3})
n'_e	number density of electrons	(ft^{-3})
n'_+	number density of ions	(ft^{-3})
p'	pressure	(lb/ft^2)
Q	$= r_i/d\alpha/dt$	(dimensionless)
r_i	rate of ionisation	(sec^{-1})
r_r	rate of recombination	(sec^{-1})
s'	specific entropy	(ft lb/°K)

T'/

T'	plasma or atom temperature	(°K)
T'_e	electron temperature	(°K)
T'_{exc}	first electronic excitation potential	(°K)
v'	velocity	(ft/sec)
x'	distance measured from throat as datum	(ft)
α	ionisation fraction = $n_e/n_e + n_a$	(dimensionless)
γ	ratio of specific heats = C_p/C_v	(dimensionless)
ζ	dimensionless distance measured from the throat as datum	
ρ'	density	(slugs/ft^3)
χ	ionisation potential	(ft lb)

Suffices

i	ionisation quantities
o	stagnation quantities
e	electron quantities
eq	equilibrium quantities

Primes denote dimensional quantities.

Superfix * denotes throat conditions.

---

1. Introduction

One of the most recent additions to the facilities available for similating high velocity flight is the plasma jet wind tunnel (Ref.1). This device creates a plasma - an ionised gas - in an arc chamber and then expands it through a nozzle into a vacuum chamber. In this manner very high stagnation enthalpies may be obtained and the flow may be expanded to hypersonic velocities. The great advantage of the plasma jet wind tunnel is that it may be run for comparatively long periods. However, this means that the power to drive the plasma jet must be supplied continuously, and in order to keep the power requirements down comparatively low stagnation pressures are normally employed. Conditions in the plasma tunnel therefore consist of a high temperature gas stream at low pressure, rapidly expanding to a very high velocity; these are exactly the conditions required to produce departures from equilibrium, and so-called relaxation effects. Relaxing gas flows are sensitive to the density, as this affects the rate of collision between particles of the different species, and hence the rate of return to equilibrium. Particularly severe relaxation effects must

monatomic gas through a nozzle. The thermodynamic equations for such a gas are very similar to those for a partially dissociated diatomic gas. It may therefore be expected that the ionic recombination process considered in this report will be broadly similar to the atomic recombination in nozzles studied previously by Bray (Ref.2) and in fact the present work attempts to follow the procedure of Ref.2.

However, ionic recombination is a much more complicated process than atomic recombination because electrons and ions can recombine in many ways. Also, the electrons and atoms are very well insulated from each other energetically (Ref.3) and may therefore possess widely different temperatures. An acceptable rate equation has not yet been found, and so the present paper does not attempt a step-by-step interpretation of the one-dimensional flow equations with a finite rate of ionic recombination, in the manner described in Ref.2 for the case of atomic recombination.

In section 2 the concept is introduced of an ideal ionising monatomic gas in equilibrium, analagous to Lighthill's ideal dissociating gas (Ref.4) and the equations of state and a Mollier diagram for this gas are given. Rate equations for ionisation and recombination are discussed in the next section, and the results of Bond (Ref.5) and Petschek and Byron (Ref.3) on strong shock waves in argon are given in a suitable form for our use. Section 4 deals with the integration of the quasi-one-dimensional flow equations for the limiting cases of equilibrium and complete freezing, and numerical results are given for these cases using the ideal ionising gas. The final section deals with conditions under which the flow may be expected to depart from equilibrium, using an analysis similar to that developed in Ref.2 in which freezing is related to the relative magnitudes of the gross and nett rates of recombination. The rate constants for argon, deduced in the manner discussed in section 3, are employed here. Also a criterion for the flow to be adiabatic is discussed briefly.

The basic assumptions in the present work are very similar to those in Ref.2; in particular, the flow is assumed to be one-dimensional, steady and inviscid. Magneto-fluid-dynamical effects which may arise near the electrodes of a plasma jet are neglected here. Ionisation resulting from the electric field in the arc chamber is also neglected, and it is assumed that expansion of the hot gases takes place from a large reservoir in which equilibrium conditions prevail. Ionisation and recombination on the walls of the nozzle are not considered.

The physical processes involved in the expansion of high temperature argon through a nozzle are undoubtedly very complicated, and the authors do not wish to suggest that the present very simple analysis will give realistic results. The neglecting of important effects, such as the temperature difference between the electrons and the atoms, the conductivity of the electron gas, magneto-gas-dynamic forces and nozzle wall effects may lead to serious errors.

2. The Ideal Monatomic Gas in Equilibrium

The thermodynamic equations used in this section have been developed in the same manner as those for the ideal dissociating gas (Ref.2), and it is therefore an ideal ionizing monatomic gas which is being studied. The majority of the equations have been formulated by Frood (Ref.6) and hence detailed derivations will not be included here.

The thermal equation of state for a mixture of neutral atoms, ions and electrons, each of which behave as a perfect gas is:

$$p' = n' k T' (1 + \alpha) \qquad \ldots (1)$$

where n' = number density of atomic nuclei and is given by:

$$\rho' = m n' \qquad \ldots (2)$$

where/

where m = mass of an atom

α = degree of ionisation defined by:

$$\alpha = \frac{n'_e}{n'_e + n'_a} \qquad \ldots (3)$$

n'_e = number density of electrons

n'_+ = number density of ions since the gas is assumed to be electrically neutral

n'_a = number density of atoms

and $n' = n'_a + n'_e$.

The primes denote dimensional quantities, unprimed symbols will be used later to represent suitably defined dimensionless quantities.

The law of mass action, or Saha equation governing the equilibrium composition of electrons, ions and neutral atoms is:

$$\frac{\alpha^2}{1-\alpha} = \frac{1}{n'} B' T'^{\frac{3}{2}} e^{-\chi/kT'} \qquad \ldots (4)$$

where $B' = 8.307 \times 10^{20}$ ft^{-3} °K$^{-\frac{3}{2}}$

χ = ionisation potential of the gas.

This expression is for the single ionisation of a perfect gas and neglects electronic excitation of the atoms and ions.

The expressions for internal energy per unit mass and specific enthalpy follow quite simply if electronic excitation and double ionisation are neglected. They are:

$$u' = \frac{3}{2}(1+\alpha)\frac{k}{m}T' + \alpha\frac{\chi}{m} \qquad \ldots (5)$$

and

$$i' = \frac{5}{2}(1+\alpha)\frac{k}{m}T' + \alpha\frac{\chi}{m}. \qquad \ldots (6)$$

It is seen that as α approaches zero at low temperatures the ideal ionising gas becomes a perfect monatomic gas with constant specific heats and $\gamma = 5/3$ as would be expected.

Table 1/

Table 1

Percentage errors in the Saha and energy equations for argon, due to neglect of the first excited state of ions

T (°K)	% Error in B'	% Error in (χ/k)
0.00	50.00	0.00
2063	26.67	0.175
5000	12.78	0.279
10,000	6.76	0.326
15,000	4.53	0.345
20,000	3.45	0.350

Table 1 shows the percentage error in the quantity B' in equation (4) introduced by neglecting the first excited state of the ions, for the case of argon. Excitation of the atoms will have a smaller effect. It is seen that the error becomes comparatively large at low temperatures, but under these conditions $\alpha \to 0$ and so equation (4) is not required. This equation also fails at very high temperatures due to multiple ionisation and higher excited states, but in the range of interest (say $10{,}000 < T' < 20{,}000°K$) the error is small. Table 1 also shows the error involved in neglecting the effect of the first excited state on the quantity χ/k in the energy equation; this error is seen to be small under all conditions. Of course, the internal energy is also affected by the error in α, but this is acceptable under conditions of interest. Similar results are obtained for other monatomic gases.

The equations (1), (4), (5) and (6) may now be non-dimensionalised by a similar method to that used by Lighthill (Ref.4) for the ideal dissociating gas. For this purpose a characteristic temperature, density, pressure, internal energy and velocity are defined for the plasma: (Values of these properties for argon are given in Table 2)

$$\left.\begin{aligned} T_i' &= \chi/k \\ \rho_i' &= B' m \left(\frac{\chi}{k}\right)^{\frac{3}{2}} \\ p_i' &= \rho_i' \left(\frac{\chi}{m}\right) \\ u_i' &= \chi/m \\ v_i' &= \sqrt{\chi/m} \end{aligned}\right\} \quad \ldots (7)$$

The main differences between these quantities and those used by Lighthill is in the expression for the characteristic density. It was stated by Frood (Ref.6) that the concept of characteristic density could

not/

not apply to an ionising gas, because such a density, far from being constant, would vary as temperatures to the three halves. Whilst this is certainly true if the characteristic density is defined in precisely the same way as Lighthill defines it, a characteristic density may in fact be defined by retaining the $T^{\frac{3}{2}}$ term in the Saha equation and making the temperature dimensionless by taking (χ/k) as a unit. The remaining constant on the right-hand side of the Saha equation then has the dimensions of density. There is no loss of accuracy by doing this and the other equations may then be non-dimensionalised quite easily.

Equations (1), (4), (5) and (6) may now be written in terms of the dimensionless quantities T, ρ, p, u and i using the characteristic ionisation quantities as units.

$$p = \rho T (1 + \alpha) \qquad \ldots (8)$$

$$\frac{\alpha^2}{1 - \alpha} = \frac{1}{\rho} T^{\frac{3}{2}} e^{-1/T} \qquad \ldots (9)$$

$$u = \frac{3}{2} (1 + \alpha) T + \alpha \qquad \ldots (10)$$

$$i = \frac{5}{2} (1 + \alpha) T + \alpha \qquad \ldots (11)$$

Table 2

Characteristic ionisation quantities for argon

Quantity	Units	Value for Argon
T_i'	°K	1.821×10^5
ρ_i'	slugs/ft^3	2.9326×10^{-3}
p_i'	lb/ft^2	1.1976×10^{11}
u_i'	ft lb/slug	4.0836×10^8
v_i'	ft/sec	2.0208×10^4

Equations (8), (9) and (10) completely specify the thermodynamic behaviour of the ideal ionising monatomic gas in the range of conditions where electronic excitations and double ionisation may be neglected. The first significant deviation will occur either at temperatures low enough for the error in the quantity B to be large or at temperatures high enough for double ionisation to be important. For the low temperature

example. This is to be expected in the range of temperatures under consideration and Lighthill (Ref.4) drew attention to the same phenomenon in the case of the ideal dissociating gas. The Mollier diagram in that case is, in fact, very similar to the one presented here, and in both cases the perfect gas conditions are met at the low temperature end of the diagram. The constant of integration encountered in the entropy equation has been taken as zero.

3. Discussion of the Rate Equation

The theory of ionisation rates is not sufficiently advanced at present to provide a general rate equation for the ideal ionising monatomic gas in cases where equilibrium is not achieved. Ionisation is a more complicated process than dissociation because there are many different mechanisms which can produce free electrons, and it is not certain which will be the most important in given circumstances. Also the collision cross-sections for the various reactions may differ by orders of magnitude, and the electron temperature may be very different from the atom temperature.

Detailed studies of ionisation rates behind shock waves in argon have been carried out by Bond (Ref.5) and Petschek and Byron (Ref.3). The information required for the final section of this paper will be obtained by combining the results of these three workers with the condition that the Saha equation (equation (4)) must be obeyed when the gas is in equilibrium. In this way information about recombination rates may be obtained from ionisation rate data, but there are flaws in the argument, as explained later. It must be emphasised here that although the dimensionless quantities for the ideal ionising gas are used for convenience, there is no evidence that the rate constants of this section apply to gases other than argon.

Other work on a rate equation for argon has been carried out by Weymann (Ref.7) and Alphar and White (Ref.8). Their results do not agree in every respect with Refs.3 and 5.

Bond (Ref.5) has suggested that of all the reactions giving rise to ionisation and recombination only three need to be considered, namely:

$$A + A \underset{\alpha_1}{\overset{\beta_1}{\rightleftharpoons}} A + A^+ + e \qquad \ldots (12)$$

$$A + e \underset{\alpha_2}{\overset{\beta_2}{\rightleftharpoons}} A^+ + 2\,e \qquad \ldots (13)$$

$$A + h\nu \underset{\alpha_3}{\overset{\beta_3}{\rightleftharpoons}} A^+ + e \qquad \ldots (14)$$

These three reactions represent ionisation by atom - atom, atom - electron and atom - photon collisions respectively, together with the corresponding recombination processes. Petschek and Byron (Ref.3) have shown that the atom electron collisions (equation (13)) are by far the largest source of ionisation providing there are sufficient electrons present in the gas, and that about 90% of the total ionisation behind a strong shock wave comes from this reaction. They have also shown that atom - atom collisions lead to a low rate of ionisation, and that the ionisation rate at low electron densities, when atom - electron collisions are rare, is probably dominated by impurity levels rather than by equation (12). It follows that equation (12) will probably also lead to a relatively low rate of recombination, and it is therefore suggested that in the formulation of a rate equation suitable for use in this paper this reaction may be neglected altogether.

Equation (14)/

Equation (14) describes a two-body recombination process, whereas equations (12) and (13) give three-body recombinations; it follows that equation (14) will become more important at low densities where three-body collisions are very rare. However, it is suggested that the atom - photon ionisation may be neglected, if it is assumed that the photons produced in the two-body recombinations are always emitted as radiant energy. The photon density level in the gas is therefore always low, and equation (14) proceeds only from right to left. This assumption was also made by Bond.

It seems possible therefore that in the present application the only reactions which need be considered are:

$$A + e \underset{\alpha_2}{\overset{\beta_2}{\rightleftharpoons}} A^+ + 2\,e \qquad \ldots (13)$$

$$A + h\nu \xleftarrow[\alpha_2]{} A^+ + e \qquad \ldots (15)$$

With these approximations the plasma will never be strictly in equilibrium because equation (15) is not balanced, and by the law of microscopic reversibility, when the plasma is in equilibrium each individual reaction must balance; it is also apparent that the flow will never be exactly adiabatic, as each two-body recombination leads to the removal of an energy ($h\nu$) from the system in the form of radiation. These limitations will be discussed later.

Equations (13) and (15) yield a nett rate of ionisation which may be written:

$$\frac{dn'_e}{dt} = \beta_2\, n'_a\, n'_e - \alpha_2\, n'^3_e - \alpha_3\, n'^2_e \qquad \ldots (16)$$

following Bond's analysis, and the use of the condition that equation (13) must reduce to the Saha equation in equilibrium gives a relationship between β_2 and α_2, the production and recombination coefficients respectively. We shall use this equation in the form:

$$\frac{d\alpha}{dt} = r_i - r_r$$

where r_i is the rate of ionisation (corresponding to the term containing β_2 in equation (16)), and r_r is the rate of recombination (the sum of the terms containing α_2 and α_3).

Petschek and Byron have discussed the atom-electron reaction (equation (13)) in some detail in connection with their shock tube work. For this case they have considered the reaction to proceed only in the ionisation direction, so that the approach to a final equilibrium ionisation level behind the shock wave cannot be predicted by their method. They have suggested as a possible mechanism for atom - electron ionisation that atoms are first raised to their first excited state by collision with electrons, and that all of the atoms excited in this manner are later ionised, so that the ionisation rate is the same as the rate of excitation. Choice of a suitable empirical law for the inelastic cross-section for this reaction then gives:

$$r_i = A' n_e \left[\frac{2(kT'_e)^3}{\pi m_e}\right]^{\frac{1}{2}} \left(\frac{T'_{exc}}{T'_e} + 2\right) e^{-T'_{exc}/T'_e} \qquad \ldots (17)$$

where $A' \left[\frac{2k^3}{\pi m_e} \right]^{\frac{1}{2}} = 6.677 \times 10^{-21} (ft^3/sec)\ (°K)^{-\frac{3}{2}}$

for the rate of ionisation by reaction (13), where T_{exc} is the energy of the first excited state of argon expressed in °K ($T_{exc} = 1.340 \times 10^5$ °K), T_e is the undetermined electron temperature, and a factor $(1 - \alpha)$ has apparently been omitted from the right-hand side because Petschek and Byron assume that $\alpha << 1$. They then proceed to set up an energy balance for the electrons, in order to determine the electron temperature T_e. In this they neglect the rate of change of the thermal energy of the electrons, which they show to be small in their case, and also the rate of gain of energy due to the inelastic collisions involving recombination. The rate of transfer of energy to the electrons in elastic collisions they deduce to be:

$$Q_{el} = \frac{n_e'^2\ e^4}{m_a} \left(\frac{8\pi m_e}{kT_e'} \right)^{\frac{1}{2}} \left(\frac{T_a'}{T_e'} - 1 \right) \ell n \left(\frac{9(kT_e')^3}{8\pi n_e' e^6} \right) \qquad \ldots (18)$$

and the rate of loss of energy due to inelastic collisions involving ionisation is, from equation (17):

$$Q_{in} = A' \left(\chi + \frac{5}{2} kT_e' \right) n_e' n_a' \left[\frac{2(kT_e')^3}{\pi m_e} \right]^{\frac{1}{2}} \times \left(\frac{T_{exc}'}{T_e'} + 2 \right) e^{-T_{exc}'/T_e'} \qquad \ldots (19)$$

neglecting recombination their energy balance is:

$$Q_{el} = Q_{in} \qquad \ldots (20)$$

and this gives the required relationship between T_a, T_e and α. However, since recombination is neglected, equation (20) yields an electron temperature which is always less than or equal to the atom temperature, a situation which is applicable to the ionising gas behind a shock wave but not to the recombining plasma considered here. In order to allow the electron temperature to be greater than the atom temperature, the energy balance of equation (20) must include another term to take account of recombination. This step will not be taken in the present report as we are mainly interested here in a criterion for the maintenance of equilibrium, which requires an expression for the rate of ionisation under equilibrium conditions. For this purpose we shall assume that $T_a = T_e$ so that equation (17) gives the ionisation rate directly. It is hoped to explore the effect of differing atom and electron temperatures in a later work.

Once an expression for r_i has been found the rate of three-body recombination follows at once from the condition that equation (13) must balance at equilibrium, when the Saha equation (equation (14)) applies. The three-body contribution to r_r is therefore

$$r_i \frac{\alpha^2}{1 - \alpha} \frac{n'}{B'} T'^{-\frac{3}{2}} e^{\chi/kT'} \qquad \ldots (21)$$

where T' is assumed to be the atom temperature rather than the electron temperature.

No experimentally checked data on rates of recombination through the two-body collision process of equation (15) have been found. However, Bond (Ref.5) gives an estimated value for the recombination coefficient α_3 for argon, obtained from the wave equation for hydrogen. This is

$$\alpha_3 = D\, T'^{-\frac{1}{2}} \qquad \ldots (22)$$

where $D = 7.609 \times 10^{-15}$ (ft^3/sec) $^\circ K^{\frac{1}{2}}$.

Finally, the rates of ionisation and recombination may be written in terms of the dimensionless quantities defined in Section 2, using equations (17), (21) and (22) and assuming a simple collision theory model for the two-body recombination. The results are

$$r_i = A\,\rho\,\alpha(1-\alpha)\,T_e^{\frac{3}{2}}\left(\frac{T_{exc}}{T_e}+2\right)e^{-T_{exc}/T_e} \qquad \ldots (23)$$

$$r_r = B\,\rho^2\,\alpha^3\left(\frac{T_e}{T}\right)^{\frac{3}{2}}\left(\frac{T_{exc}}{T_e}+2\right)e^{\left(\frac{1}{T}-\frac{T_{exc}}{T_e}\right)} - E\,\rho\,\alpha^2\,T^{-\frac{1}{2}} \qquad \ldots (24)$$

where $A = B = 3.349 \times 10^{16}$ sec^{-1}

$E = 1.151 \times 10^{13}$ sec^{-1}

and $T_{exc} = \dfrac{T'_{exc}}{\chi/k} = 0.7359$.

To evaluate these expressions we require a relationship between T_e and T, as discussed above.

4.1 Quasi-one-dimensional flow equations

The frictionless adiabatic flow of an ideal ionising monatomic gas through a duct of slowly varying cross-sectional area A' is described by the equations of conservation of mass, momentum and energy:

$$\rho\, v\, A' = \rho^*\, v^*\, A^* = \psi \qquad \ldots (25)$$

$$v\frac{dv}{dx'} + \frac{1}{\rho}\frac{dp}{dx'} = 0 \qquad \ldots (26)$$

$$i + \tfrac{1}{2}v^2 = i_o \qquad \ldots (27)$$

(in which asterisks denote throat conditions), together with the thermodynamic relationships of equations (8) and (11) and a rate equation. In general these equations cannot be solved until a nozzle shape has been specified, and procedure here follows precisely that used in the dissociation case (Ref.2) a nozzle with a hyperbolic area distribution being chosen:

$$A' = A^* + K^2 (x')^2$$

An area ratio is defined by

$$A = A'/A^*$$

and a dimensionless distance by

$$\zeta = \frac{K_N x'}{\sqrt{A^*}}$$

so that the nozzle shape becomes:

$$A = 1 + \zeta^2 . \qquad \ldots (28)$$

This equation together with the five equations given above and a rate equation yield a set of seven equations with a similar number of unknowns, and the flow through the nozzle may therefore be solved. Since a useable rate equation has not been established the solution will not be attempted here. The equilibrium and frozen flow cases will, however, be solved and the methods employed will now be discussed.

4.2 Equilibrium flow

It may be shown from the law of mass action and the condition that the flow is isentropic that:

$$\frac{1+\alpha}{T} + \frac{5}{2}\alpha + 2\ell_n\left(\frac{\alpha}{1-\alpha}\right) = f(\alpha_o, T_o) = \text{constant} \qquad \ldots (29)$$

or

$$T = \frac{1+\alpha}{f - \frac{5}{2}\alpha - 2\ell_n\left(\frac{\alpha}{1-\alpha}\right)} \qquad \ldots (30)$$

and from the flow equations (25) and (27) and equations (28) and (30) an expression for $d\alpha/d\zeta$ may be deduced:

$$\frac{d\alpha}{d\zeta} = \frac{\zeta}{1+\zeta^2} \cdot \frac{A(\alpha, T)}{B(\alpha)T^3 + C(\alpha)T^2 + D(\alpha)T + E(\alpha)} \qquad \ldots (31)$$

where $A(\alpha,T) = 4(i_o-i)\alpha(1-\alpha)(1+\alpha)T$

$B(\alpha) = 25\alpha(1-\alpha)(1+\alpha)+20(1+\alpha)$

$C(\alpha) = 25\alpha(1-\alpha)(1+\alpha)+10(1+\alpha)-5(1+\alpha)^2(2-\alpha) - \frac{15}{2}(i_o-\alpha)\alpha(1-\alpha)-6(i_o-\alpha)$

$D(\alpha) = 6\alpha(1-\alpha)(1+\alpha)-6(i_o-\alpha)\alpha(1-\alpha)$

$E(\alpha) = -2(i_o-\alpha)\alpha(1-\alpha) .$

This equation shows that as $\zeta \to 0$ at the sonic throat $d\alpha/d\zeta \to 0$ unless:

$$B(\alpha^*)T^{*3} + C(\alpha^*)T^{*2} + D(\alpha^*)T^* + E(\alpha^*) = 0 . \qquad \ldots (32)$$

This yields a relationship between T^* and α^* and if this equation is solved simultaneously with equation (30) then T^* and α^* may be obtained. It is then a very simple calculation which yields ρ^* and v^* and hence the mass flow rate ψ. Equations (9), (11) and (27) then yield conditions downstream of the throat; this is achieved by selecting values of α and then solving for A, T, ρ and v. The simultaneous solution of equations (30) and (32) present the major difficulty here, and because of the complexity of equation (32) the solution was performed on a digital computer.

4.3/

4.3 Frozen flow

The problem of frozen flow presents few difficulties since freezing will occur when α tends to a constant value which is greater than zero. This will occur if the recombination rate (r_r) tends to zero much faster than $\left[\frac{d\alpha}{dt}\right]_{eqn.}$ (see Section 5).

For flow which is frozen everywhere except in the reservoir upstream of the nozzle:

$$\alpha = \alpha_o = F(p_o, T_o) = \text{constant}$$

$$p = \rho T(1 + \alpha_o)$$

$$i = \frac{5}{2}(1 + \alpha_o) T + \alpha_o$$

$$e = \frac{3}{2}(1 + \alpha_o) T + \alpha_o$$

and it is seen that these equations are analagous to those for a perfect gas with

$$R \equiv (1 + \alpha_o)$$

$$C_p \equiv \frac{5}{2}(1 + \alpha_o)$$

$$C_v \equiv \frac{3}{2}(1 + \alpha_o)$$

and $$\gamma = \frac{C_p}{C_v} = \frac{5}{3} = \text{constant.}$$

The frozen flow parameters may therefore be obtained from normal supersonic flow theory for a perfect gas with $\gamma = 5/3$, whence:

$$\frac{T_o}{T} = \left(1 + \frac{\gamma - 1}{2} M_c^2\right) = \left(1 + \frac{1}{3} M_c^2\right)$$

$$\frac{p_o}{p} = \left(1 + \frac{\gamma - 1}{2} M_c^2\right)^{\gamma/\gamma-1} = \left(1 + \frac{1}{3} M_c^2\right)^{\frac{5}{2}}$$

$$\frac{\rho_o}{\rho} = \left(1 + \frac{\gamma - 1}{2} M_c^2\right)^{1/\gamma-1} = \left(1 + \frac{1}{3} M_c^2\right)^{\frac{3}{2}}$$

$$\frac{A}{A^*} = \frac{1}{M_c}\left[\frac{3}{4}\left(1 + \frac{\gamma - 1}{2} M_c^2\right)\right]^{\frac{1}{2}\left(\frac{\gamma+1}{\gamma-1}\right)} = \frac{1}{M_c}\left[\frac{3}{4}\left(1 + \frac{2}{3} M_c^2\right)\right]^2.$$

The Mach number M_c is based on the frozen speed of sound which is given by:

$$c = \sqrt{\frac{5}{3}(1 + \alpha_o) T}$$

whence $M_c = v/c$ can be determined.

Note/

Note that it is implicitly assumed in this section that $T = T_e$, although in fact the electron and atom temperatures may be very different in frozen flow. This problem requires further study.

Table 3

Stagnation Quantities

Quantity	Dimensionless Value	Dimensional Value	Units
p_o	10^{-9}	0.83173	lb/in^2.
p_o	10^{-8}	8.3173	lb/in^2.
p_o	10^{-7}	83.173	lb/in^2.
T_o	0.05	9.105×10^3	°K
T_o	0.06	1.093×10^4	°K
T_o	0.07	1.275×10^4	°K
T_o	0.08	1.457×10^4	°K
T_o	0.09	1.639×10^4	°K

4.4 Results

The solution to the equations for equilibrium-isentropic flow and frozen-isentropic flow have been presented graphically in Figs.2-20 for various stagnation temperatures and pressures. The equivalent dimensional values of these and other stagnation quantities are given in Table 3.

It was shown above that the frozen-isentropic flow properties are identical to those of a perfect gas, with a ratio of specific heats (γ) of 5/3; the fall in temperature downstream of the nozzle is therefore unaffected by stagnation pressure and the temperature gradient is very large, a condition to be expected if the flow is hypersonic. Due to this rapid fall in temperature the increase in velocity is also rapid, and it approaches its maximum value asymptotically at an area ratio of approximately 100. Consequently, downstream of this point the continuity equation may be written approximately:

$$\rho A = \text{constant} = \psi/V_{max}$$

and in support of this approximation the logarithmic slope of the density curves approach -1 at an area ratio of 100. It is therefore evident that the frozen flow variables attain their limiting values at comparatively small distances downstream of the throat.

The equilibrium-isentropic flow properties deviate considerably from the corresponding frozen-isentropic flow properties, the main reason being that whilst recombination is taking place energy is being returned to the stream. This has the effect of reducing the temperature gradient, which in turn imposes modifications on the remaining flow variables. However, the temperature does not decrease steadily in all cases but falls very rapidly in a certain region of the nozzle, this region being different for various stagnation conditions. Once this region has been reached the

temperature/

temperature rapidly approaches its limiting value of zero. The explanation of this phenomenon is quite simple if one determines the ionisation fraction at the point where the slope changes suddenly; it is found in all cases that the ionisation fraction is very small at this point, and in fact downstream of this point the gas behaves as a perfect gas, and as a result the temperature gradient is large. In order to check this hypothesis perfect gas solutions have been calculated from suitable stagnation conditions and superimposed on the equilibrium-isentropic flow curves (see Figs.2, 6 and 10). The two sets of curves shown are in excellent agreement. In fact this phenomenon could have been predicted if the Mollier Chart (Fig.1) had been consulted; following an isentropic expansion on this chart the temperature falls only slowly until the lower regions are encountered, where the temperature lines become very bunched indicating a rapid fall in temperature. It must be pointed out, however, that the lower portion of the Mollier Chart was obtained from the perfect gas laws.

The effect of this sudden fall in temperature on the other flow variables is merely to make them approach their limiting values very much more quickly, prior to this the limiting values are approached very slowly as might be expected from previous investigations into dissociative recombination in nozzles. The limiting value of the velocity is greater for the equilibrium flow than for the frozen. The limiting values in question may be derived from the energy equation (equation (23)) from which the two limits are: $\sqrt{2}\, i_o$ and $\sqrt{2}\,(i_o - \alpha_o)$ for equilibrium and frozen flow respectively.

There are no sudden changes in the gradient of the density and velocity curves as there are with the temperature curves, it follows that the pressure curves (which have not been included) will have these sudden changes, as dictated by the equation of state (equation (8)).

5.1 Non-equilibrium flow

As the partially ionised gas expands through the nozzle, the density and temperature fall and so the rate of recombination is reduced. If the rate of expansion is too rapid recombination may not occur sufficiently fast to maintain equilibrium at the downstream end of the nozzle, even if the gas entered the nozzle in equilibrium. This situation may be described in the manner suggested in Ref.2, where three flow regimes are distinguished:

(1) A region of flow near to equilibrium, in which both the rate of ionisation r_i and the rate of recombination r_r are very large in comparison with the nett rate of ionisation $d\alpha/dt = r_i - r_r$, so that the equilibrium condition $r_i = r_r$ is closely satisfied. Equilibrium will then continue so long as this situation is maintained, that is so long as

$$-\frac{d\alpha}{dt} \ll r_i \,.$$

(2) A transition region, in which ρ and T have fallen sufficiently so that r_i and r_r are of the same order as $d\alpha/dt$, and there is consequently an appreciable departure from equilibrium. Once this process has begun the temperature falls more rapidly, because energy is no longer

and consequently

$$-\frac{d\alpha}{dt} \simeq r_r .$$

The ratio $Q = r_i / -\frac{d\alpha}{dt}$ may therefore be used as a measure of the state of the gas, since this ratio will be much greater than unity in the near equilibrium region, of the order of unity in the transition region and much less than unity in the region of nearly frozen flow. If the gas is very close to equilibrium then Q must be evaluated under equilibrium conditions, so for region (1) we have

$$Q_{eq} >> 1$$

where the suffix eq denotes equilibrium.

The quantity $(r_i)_{eq}$ is given by equation (23) together with the condition that $T = T_e$ when the gas is in equilibrium, and

$$\left(\frac{d\alpha}{dt}\right)_{eq} = \left(\frac{d\alpha}{d\zeta}\right)_{eq} v \sqrt{\frac{\chi}{m}} \frac{K_n}{\sqrt{A^*}}$$

from equation (7) and the definition of ζ, where $\left(\frac{d\alpha}{d\zeta}\right)_{eq}$ is given by equation (31). Q_{eq} may therefore be evaluated from the equilibrium flow results of section 4, if the nozzle parameter $\sqrt{\frac{\chi}{m}} \frac{K_n}{\sqrt{A^*}}$ is specified. In regions (2) and (3), however, Q will differ from Q_{eq} for the following reasons:

(1) Departure from equilibrium is accompanied by a reduction of $\left(-\frac{d\alpha}{dt}\right)$ below its equilibrium value: in fact $\left(-\frac{d\alpha}{dt}\right)$ approaches r_r as the flow freezes, and this approaches zero as ρ^2 for the three-body recombination, so that $\left(-\frac{d\alpha}{dt}\right) << \left(-\frac{d\alpha}{dt}\right)_{eq}$.

(2) Departure from equilibrium causes the temperature to fall sharply from its equilibrium value, because of the reduced amount of energy being returned to the flow; this will bring about a reduction in r_i because of the exponential term. However, in a non-equilibrium flow T_e will be greater than T (though presumably less than the corresponding T_{eq} for the same area ratio), and this effect will tend to limit the reduction in r_i.

We see therefore that both $\left(-\frac{d\alpha}{dt}\right)$ and r_i are reduced by freezing so that no definite statement can be made concerning the effect of freezing on Q. However, if the 'insulation' between atoms and electrons is very effective, so that $T_e \simeq T_{eq} > T$, then we shall have $Q > Q_{eq}$. In this case, the use of Q_{eq} (which can be evaluated) instead of the unknown Q in a criterion for frozen flow will be pessimistic; that is, it will predict freezing further upstream than it will actually occur. Further calculations are required to settle this point.

In the present preliminary study we shall empirically define the three flow regions by the equations:

Q_{eq}/

$$Q_{eq} > 10^{2} \quad \text{(near equilibrium)} \qquad \ldots (33)$$

$$10^{-2} < Q_{eq} < 10^{2} \quad \text{(transition)} \qquad \ldots (34)$$

$$Q_{eq} < 10^{-2} \quad \text{(near frozen)} \qquad \ldots (35)$$

where the transition region (equation (34)) has been made very large because of the uncertainty of the whole analysis. The condition that the gas is close to equilibrium if $Q_{eq} > 10^{2}$ should be very conservative, but there is more doubt about the frozen flow criterion (equation (35)) because of the unknown relationship between T_e and T.

Figs.21 and 22 show the variation of Q_{eq} with area ratio A, using the equilibrium flow calculations of Section 4 and the rate equation for argon which was discussed in Section 2. A range of stagnation temperatures has been considered but only two stagnation pressures: $p_o = 10^{-8}$ and 10^{-9}. It was found that with $p_o = 10^{-7}$ α_{eq} rapidly approached zero, so that relaxation effects were unlikely.

Three cases are shown in Figs.21 and 22:

(a) Small Nozzle:

$$\sqrt{\frac{\chi}{mA^*}}\, K_n = 7.949 \times 10^{5}$$

e.g., $d^* = 0.04$ in. $\theta = 3\frac{3}{4}^{\circ}$.

(b) Medium sized nozzle:

$$\sqrt{\frac{\chi}{mA^*}}\, K_n = 2.316 \times 10^{5}$$

e.g., $d^* = 0.20$ in. $\theta = 5^{\circ}$.

(c) Large nozzle:

$$\sqrt{\frac{\chi}{mA^*}}\, K_n = +6.385 \times 10^{4}$$

e.g., $d^* = 1.0$ in. $\theta = 7\frac{1}{2}^{\circ}$.

Of course, other cases may be considered by moving the curves up or down in proportion to $\sqrt{\frac{mA^*}{\chi}}\,\frac{1}{K_n}$.

The results for $T_o = 0.06$ fall most steeply, but this case is only of interest for small A, otherwise α is too small to be of interest. The other cases form a band of nearly parallel straight lines, with Q_{eq} becoming very small at large area ratios.

$p_o = 10^{-8}$

Here Q_{eq} lies in the transition region (i.e., $10^{2} > Q_{eq} > 10^{-2}$) for small area ratios, and the curves penetrate deeply in the frozen region for large area ratios. It appears therefore that there will be a lack of

equilibrium in the nozzle under a wide variety of conditions. It must be emphasized however that a very approximate analysis has been employed to obtain these curves, and the analysis must be most accurate when $Q_{eq} > 10^2$, that is when an equilibrium flow is indicated, in this case $d\alpha/d\zeta$ will be very near to its exact value.

$p_o = 10^{-9}$

These curves are somewhat lower than those for $p_o = 10^{-8}$, suggesting earlier freezing, as would be expected. In fact the curves downstream of the throat lie completely within the frozen region with the exception of $T_o = 0.09$ for large scale factor.

In the opinion of the authors, these calculations indicate that there will be a lack of equilibrium in the nozzle under a wide range of stagnation conditions. In view of the very approximate nature of these calculations it cannot be stated with any certainty that the flow will freeze in any region, however, there are indications that it will depart from equilibrium especially where p_o and $\sqrt{\frac{\chi}{mA^*}}\,K_n$ are small and at large area ratios. Under these conditions, errors in the calculation are very large. Increasing T_o and p_o appears to favour equilibrium, but it also increases α and so tends to increase the effect of any departure from equilibrium. A further study of the relationship between T and T_e is required before any definite conclusions may be drawn about the state of the flow, but this is beyond the scope of this paper.

5.2 Criterion for adiabatic flow

The condition chosen for the flow to be adiabatic is that the energy radiated per unit time must be small compared with the rate of change of enthalpy, so that

$$\frac{de_r}{dt} \ll \left|\frac{di}{dt}\right| \qquad \ldots (36)$$

where $\frac{de_r}{dt}$ = energy radiated per unit mass per unit time, with χ/m taken as the unit of energy. Clearly if this criterion is satisfied then the total energy radiated by a unit mass of gas on passing through the nozzle will always be much less than the total change of specific enthalpy.

Equation (36) will be used in the more convenient form

$$\frac{de_r}{d\zeta} \ll \left|\frac{di}{d\zeta}\right|$$

since, for equilibrium adiabatic flow

$$\frac{di}{d\zeta} = \left\{\frac{5}{2}(1+\alpha)\left[\frac{1}{T} + \frac{(1+\alpha)\left(\frac{5}{2} + \frac{2}{\alpha(1-\alpha)}\right)}{T^2}\right]\frac{5}{2}T + 1\right\}\frac{d\alpha}{d\zeta}$$

$$= f(\alpha, T)$$

from equations (11) and (30), and $d\alpha/d\zeta$ may be found from equation (31).

But/

But $$\frac{de_r}{d\zeta} = \frac{de_r}{dt} \frac{1}{vK_n} \sqrt{\frac{mA^*}{\chi}}$$

from equation (7) and the definition of ζ,

and $$\frac{de_r}{dt} = - h \nu \frac{dn_e'}{dt} \qquad \ldots(15)$$

where $$\frac{dn_e'}{dt} = \rho \alpha^2 T^{-\frac{1}{2}}$$

$$= (1 - \alpha) T_e^{-1/T} \text{ in equilibrium}$$

from the results of Bond (Ref.5) as quoted in equation (24). Hence

$$\frac{de_r}{dt} = - (1 - \alpha) T e^{-1/T} h \nu$$

and $$\frac{de_r}{d\zeta} = \frac{de_r}{dt} \cdot \frac{dt}{d\zeta} = \frac{de_r}{dt} \cdot \sqrt{\frac{mA^*}{\chi}} \frac{1}{K_n} \cdot \frac{1}{v} = F(\alpha, T, v)$$

and the criterion for adiabatic flow becomes:

$$F(\alpha, T, v) \ll f(\alpha, T) .$$

The quantities F and f have been calculated from the equilibrium isentropic results of Section 4 (i.e., assuming that the criterion is satisfied), and the ratio F/f has been found to lie between

$$10^{-33} \geq \frac{F}{|f|} \geq 10^{-38} \quad \text{for} \quad \nu = 10^{15} \text{ c.p.s.} \sqrt{\frac{\chi}{mA^*}} \cdot K_n = 7.949 \times 10^5$$

and $$10^{-34} \geq \frac{F}{|f|} \geq 10^{-39} \quad \text{for} \quad \nu = 10^{15} \text{ c.p.s.} \sqrt{\frac{\chi}{mA^*}} \cdot K_n = 6.385 \times 10^4$$

for the cases considered. These results confirm that the assumption of adiabatic flow is justified, at least for conditions close to equilibrium.

Freezing will tend to reduce $\left|\frac{di}{d\zeta}\right|$ in the downstream part of the nozzle where $v \simeq v_{max}$, and it may also tend to increase $de_r/d\zeta$ because of the temperature. It follows that radiated energy will be relatively more important in a freezing flow than in an equilibrium flow, but the magnitude of the figures quoted above for the equilibrium case leads one to believe that it will still be a negligibly small effect. The figures quoted by Hirschfelder, Curtis and Bird (Ref.9) confirm this conclusion.

6. Conclusions

temperatures are required to determine the properties of the relaxing flow. It is also shown that energy radiated as a result of two-body recombinations will lead to a negligible deviation from adiabatic flow.

Equilibrium and frozen flow calculations are performed for the case of an ideal ionising monatomic gas; the approach of this gas to a perfect gas as the ionisation fraction becomes small is also discussed.

Acknowledgements

The authors wish to thank Dr. J. B. Willis of the Department of Computation, University of Southampton, for his assistance with the numerical computations.

References

No.	Author(s)	Title, etc.
1	-	Bulletin and Annual Progress Report, 1959, University of Toronto Inst., Aerophysics.
2	K. N. C. Bray	Atomic recombination in a hypersonic wind-tunnel nozzle. Fluid Mech.6, 1. 1959.
3	H. Petschek and S. Byron	Approach to equilibrium ionisation behind strong shock waves in argon. Annals of Physics, Vol.1. 1957.
4	M. J. Lighthill	Dynamics of a dissociation gas. Part I. Equilibrium flow. J. Fluid Mech. 2, 1. 1955.
5	J. W. Bond, Jnr.	Structure of a shock front in argon. Physical Review, 105. 1957.
6	D. G. H. Frood	Strong shock waves in real atomic and molecular gases. A.R.D.E. Report (B) 11/59. 1959.
7	H. D. Weymann	On the mechanism of thermal ionisation behind strong shock waves. University of Maryland, Tech. Note BN-144. 1958.
8	R. A. Alphar and R. W. White	Optical refractivity of high temperature gases. II. Effects resulting from ionisation of monatomic gases. Physics of Fluids, Vol.2, No.2. 1959.
9	J. O. Hirschfelder, C. F. Curtis and R. B. Bird	Molecular theory of gases and liquids. Chapman and Hall, Ltd., London.

DS 97056/11/W761 K4 10/61 XL

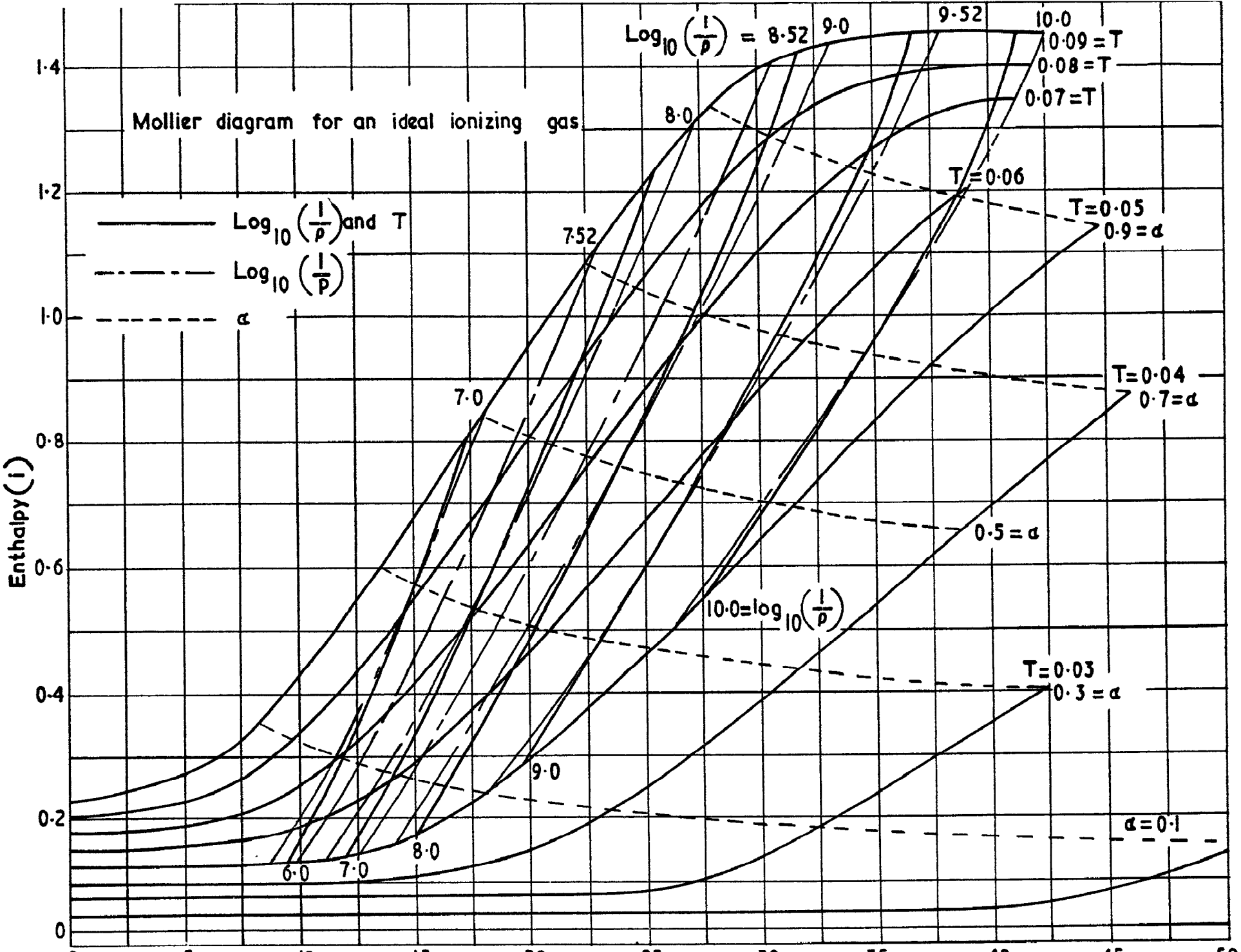
Mollier diagram for an ideal ionizing gas
Log10 (1/p) and T
Log10 (1/P)
α
Enthalpy (i)
Log10 (1/p) = 8·52
9·0
9·52
10·0
0·09 = T
0·08 = T
0·07 = T
8·0
T = 0·06
T = 0·05
0·9 = α
7·52
T = 0·04
0·7 = α
7·0
0·5 = α
10·0 = log10 (1/p)
T = 0·03
0·3 = α
9·0
α = 0·1
6·0
7·0
8·0
1·4
1·2
1·0
0·8
0·6
0·4
0·2
0

FIG. 1.

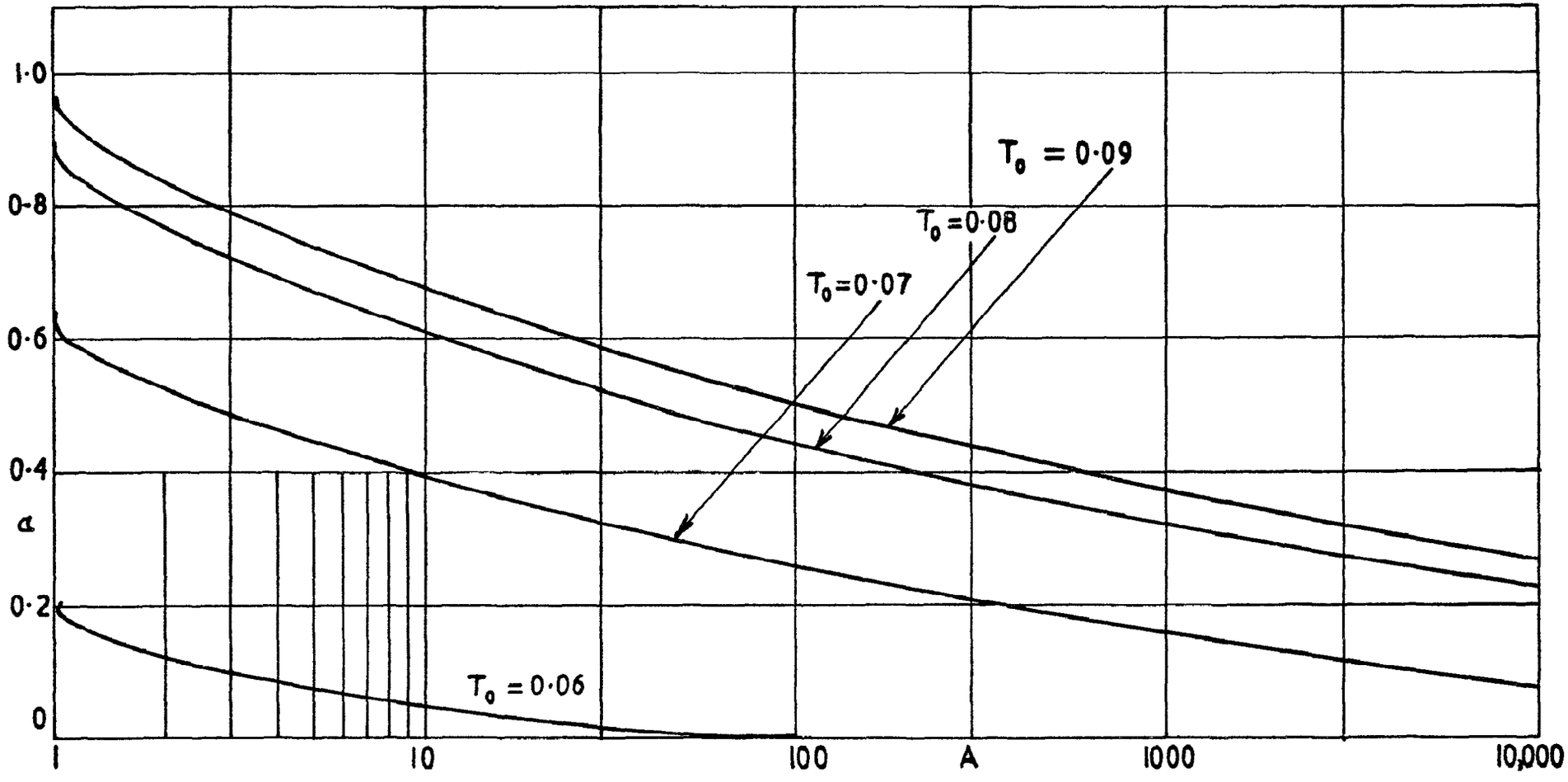

Equilibrium – Isentropic flow $p_0 = 10^{-9}$

FIG. 2.

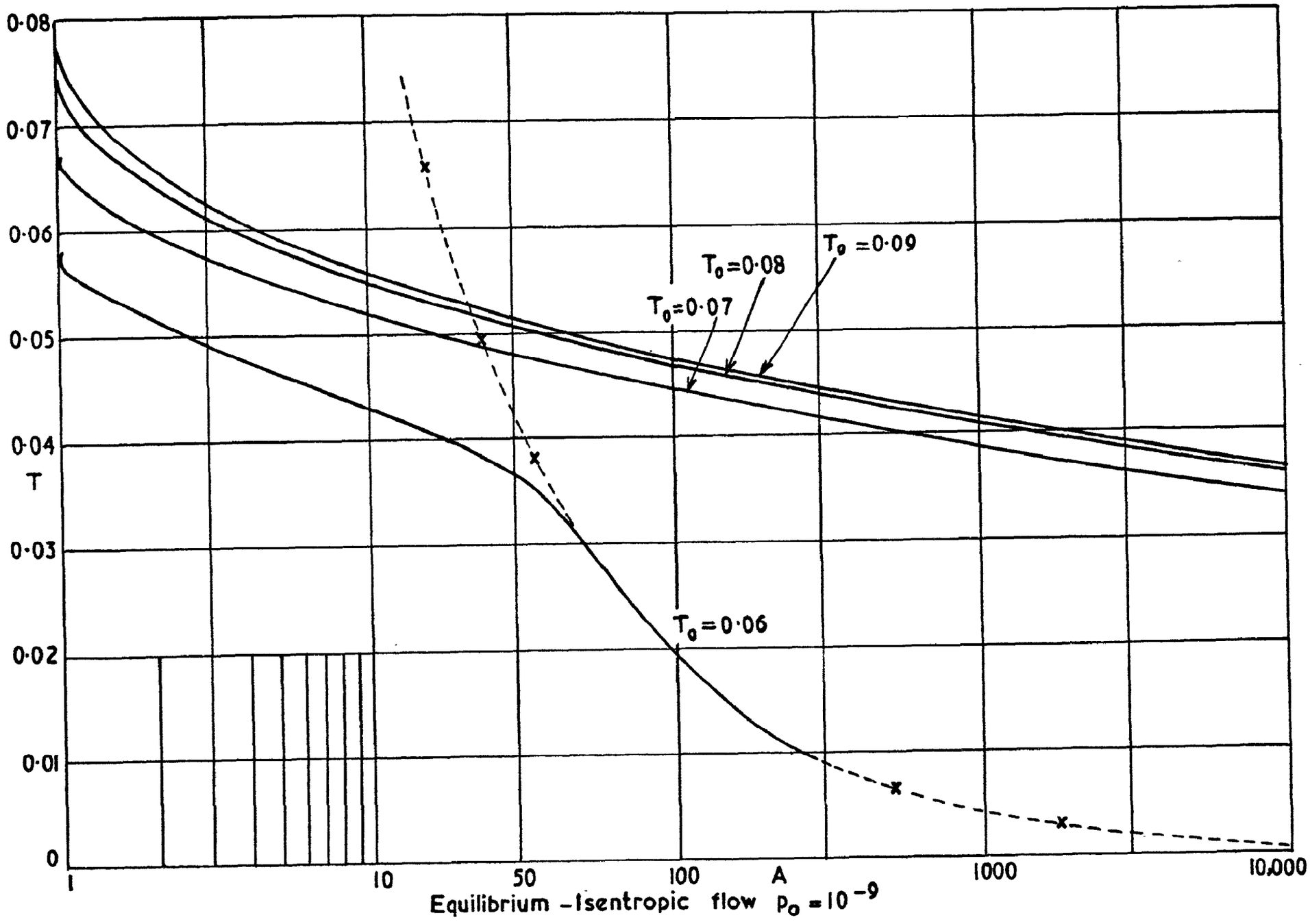
0·08
0·07
0·06
0·05
0·04
T
0·03
0·02
0·01
0
$T_0 = 0·09$
$T_0 = 0·08$
$T_0 = 0·07$
$T_0 = 0·06$
1
10
50
100
A
1000
10,000
Equilibrium – Isentropic flow $p_0 = 10^{-9}$

FIG. 3.

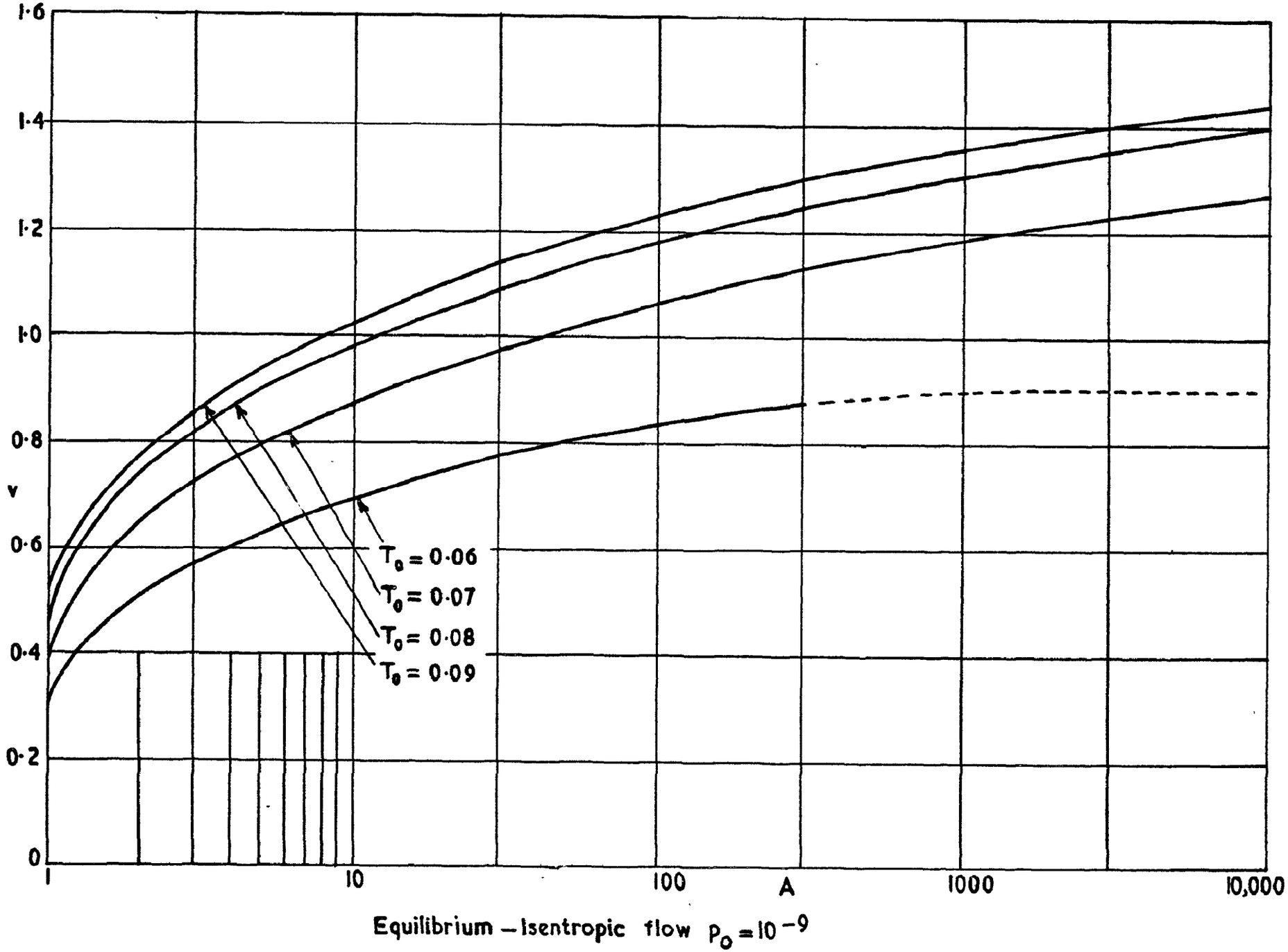
1·6
1·4
1·2
1·0
0·8
v
0·6
0·4
0·2
0
1
10
100
A
1000
10,000
$T_0 = 0·06$
$T_0 = 0·07$
$T_0 = 0·08$
$T_0 = 0·09$
Equilibrium – Isentropic flow $P_0 = 10^{-9}$

FIG. 4.

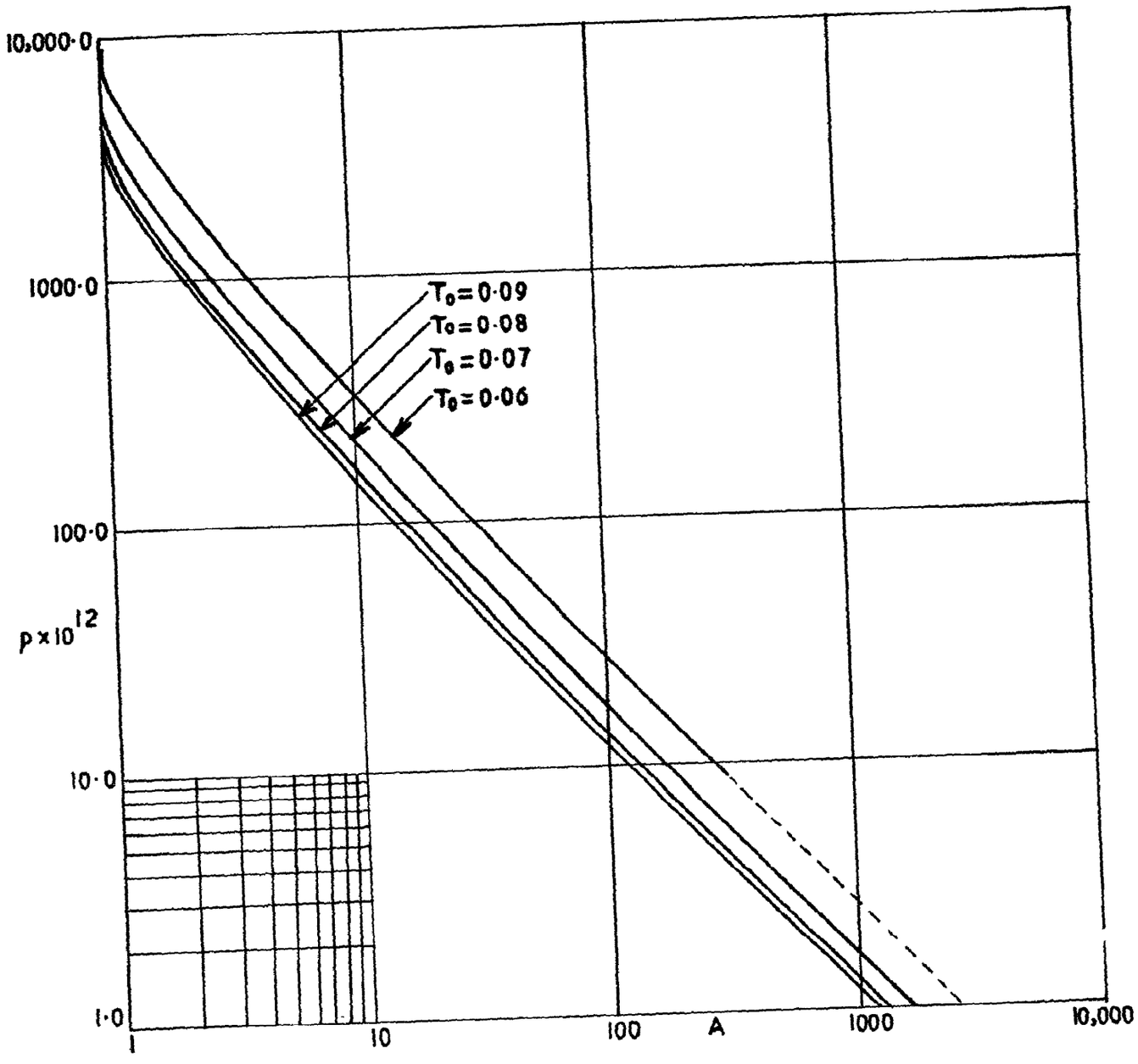

Equilibrium – Isentropic flow $p_0 = 10^{-9}$

FIG. 5.

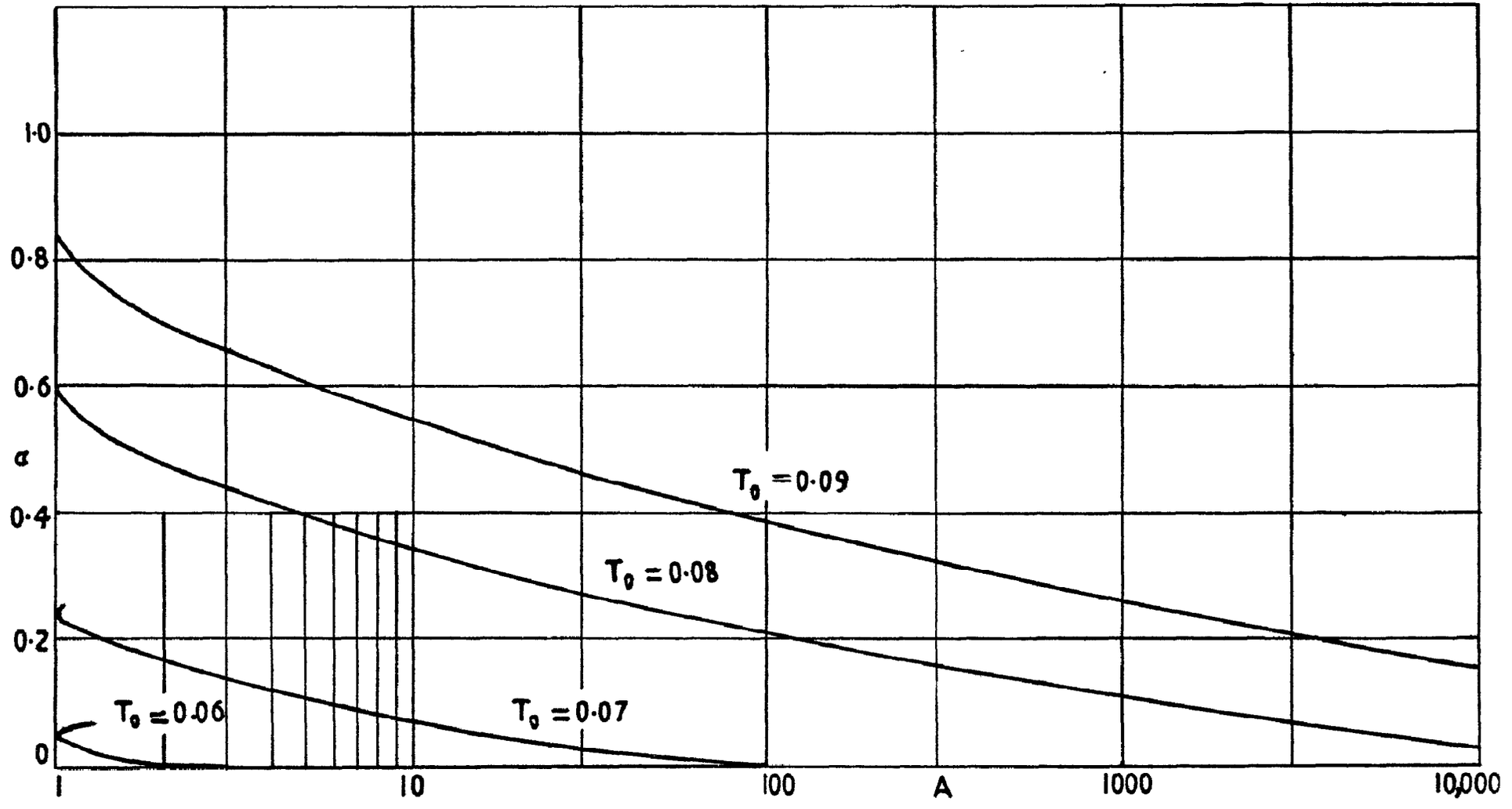

FIG. 6

Equilibrium – isentropic flow $p_0 = 10^{-8}$

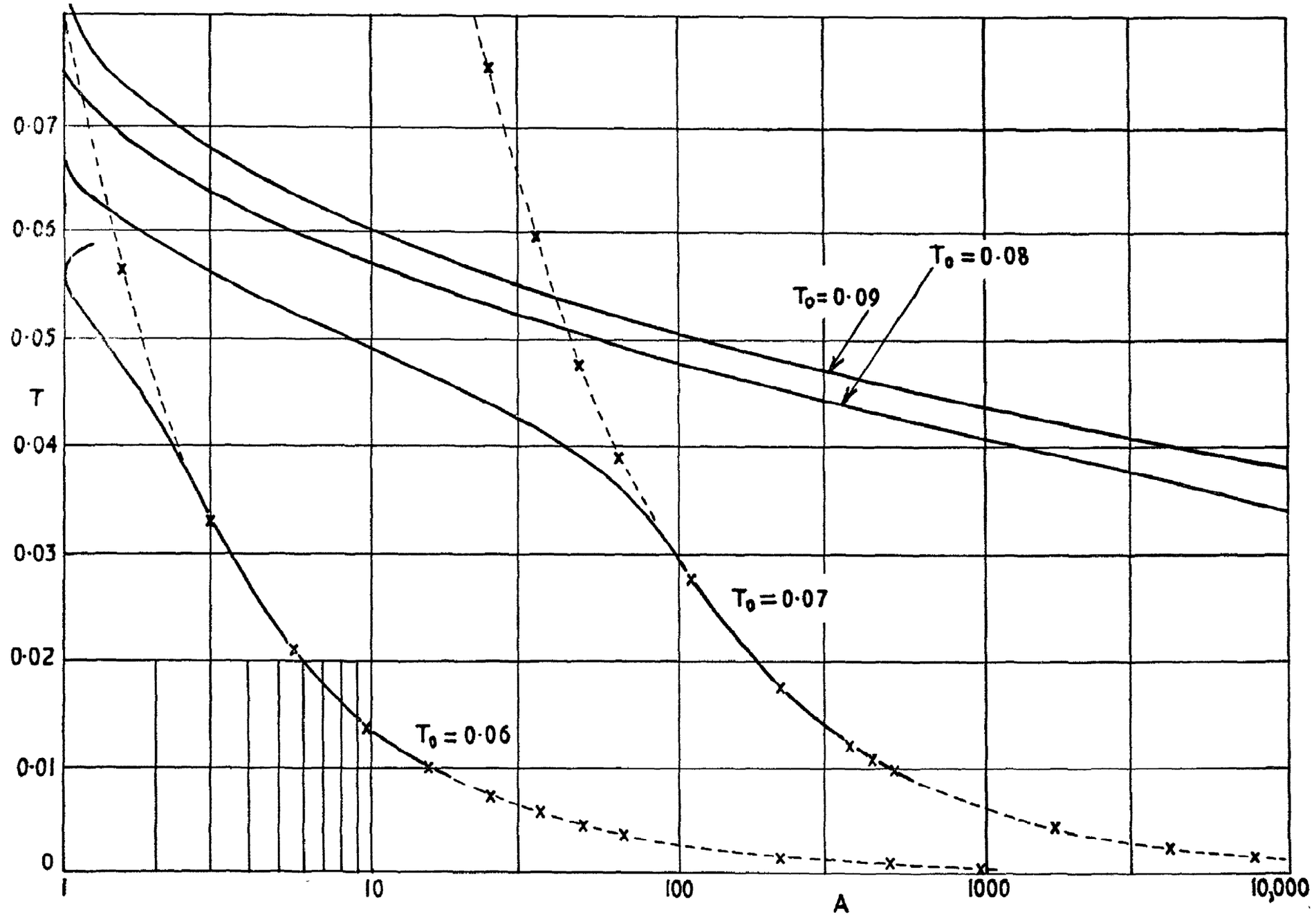

--x-- Perfect gas $\gamma = 5/3$

Equilibrium — isentropic flow $p_- = 10^{-8}$

FIG.7.

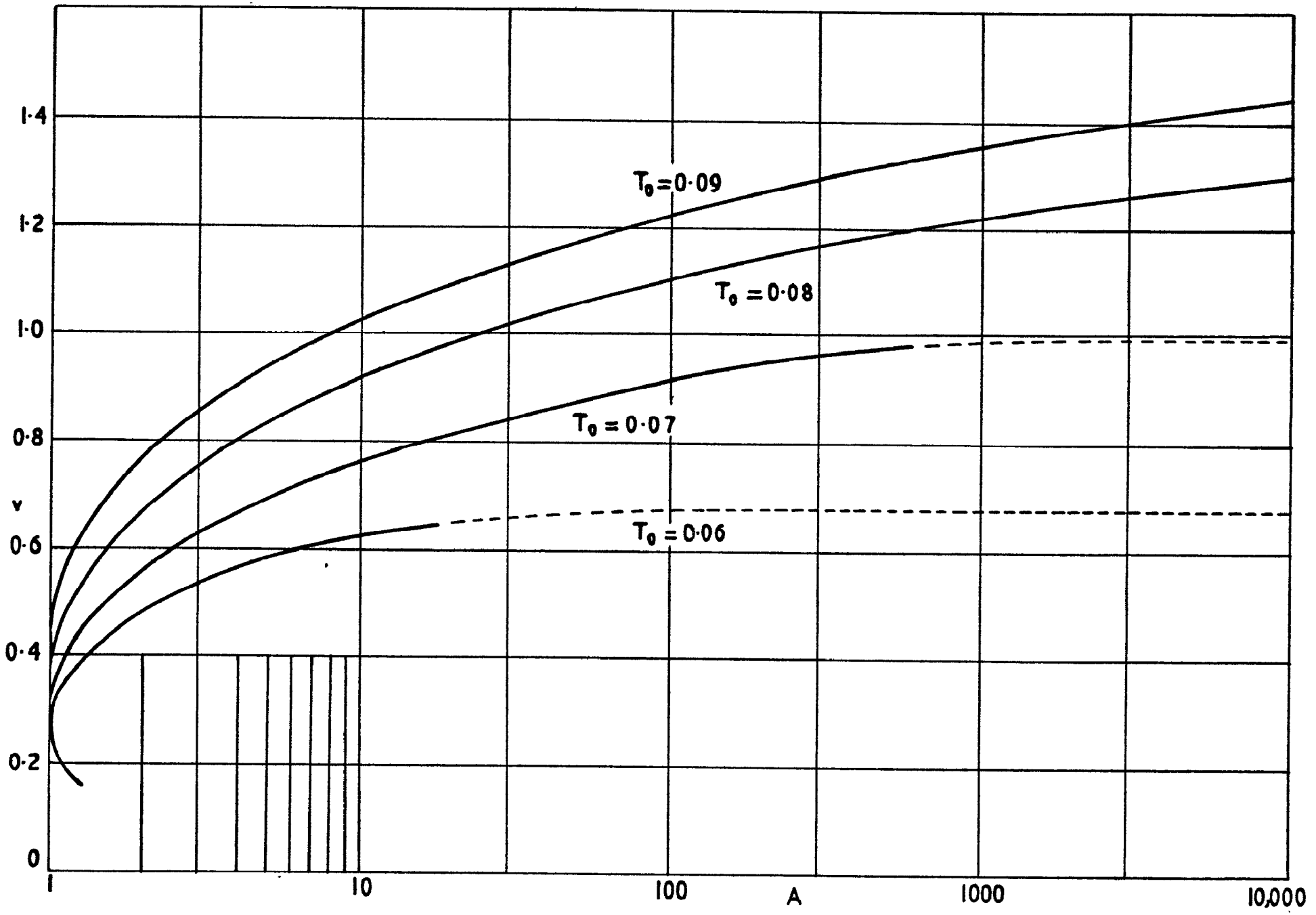
1·4
1·2
1·0
0·8
v
0·6
0·4
0·2
0
1
10
100
A
1000
10,000
$T_0 = 0·09$
$T_0 = 0·08$
$T_0 = 0·07$
$T_0 = 0·06$

FIG.8

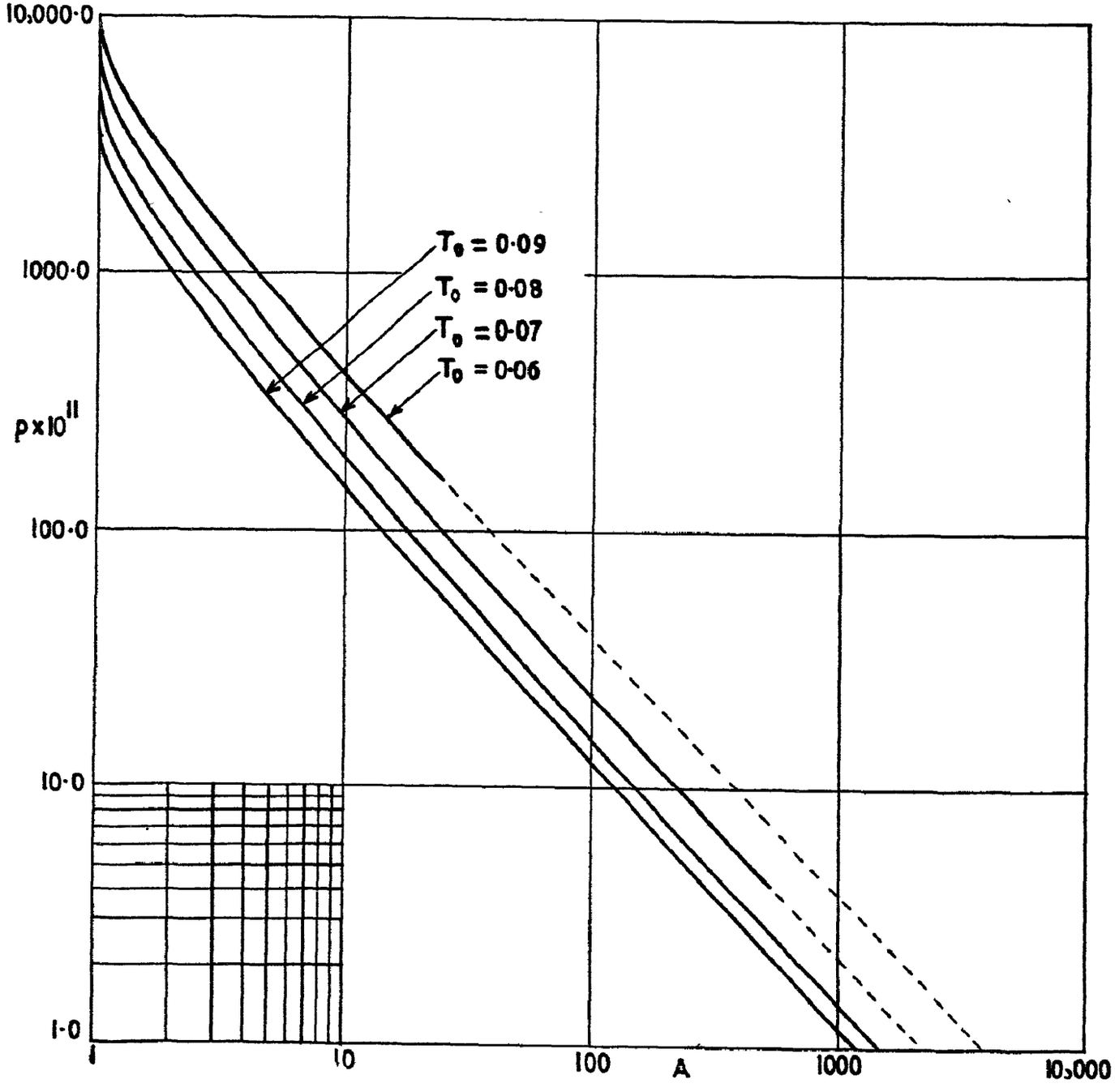

Equilibrium – Isentropic flow $p_o = 10^{-8}$

FIG. 9.

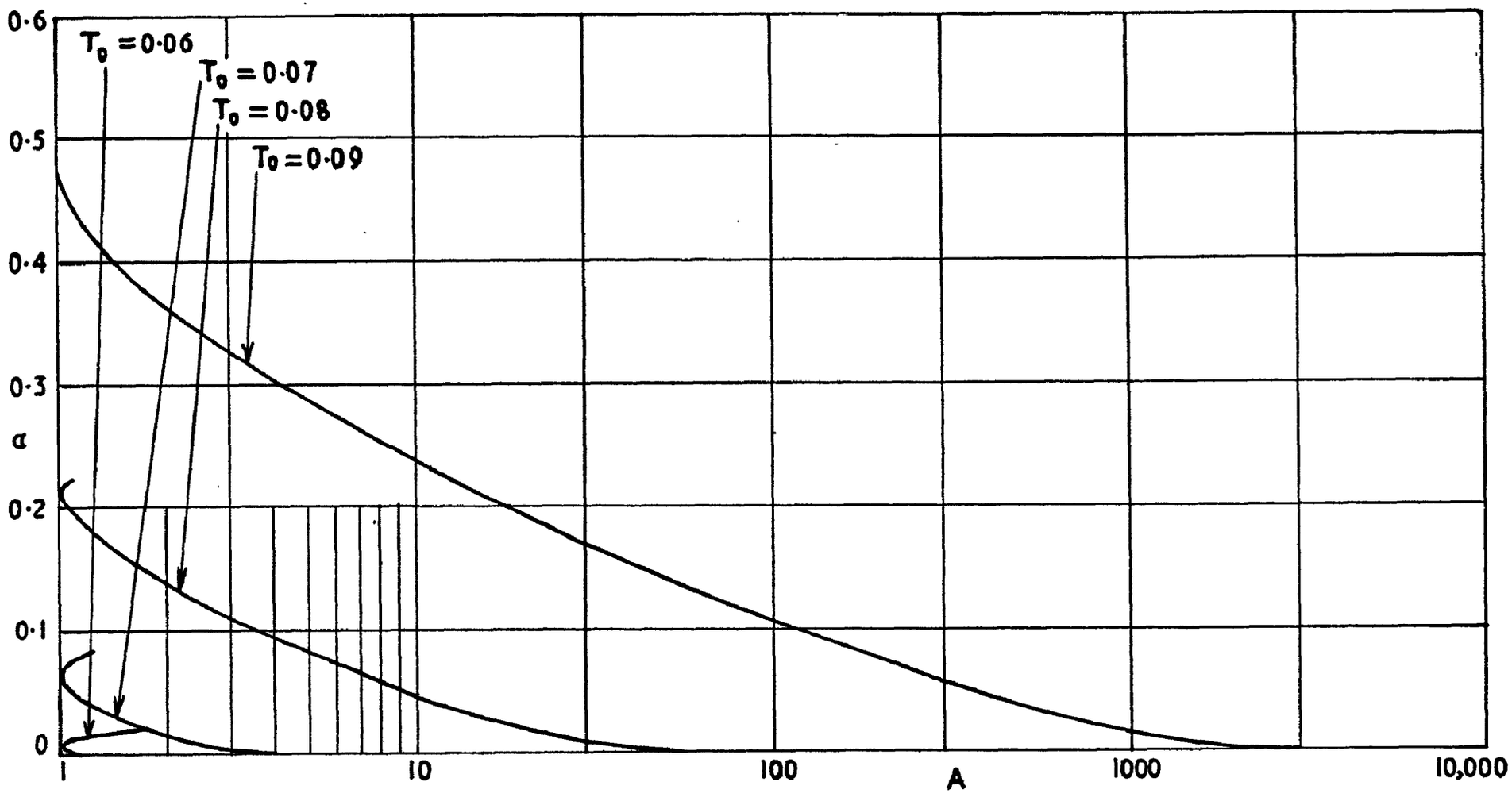

FIG.10.

Equilibrium – isentropic flow $p_0 = 10^{-7}$

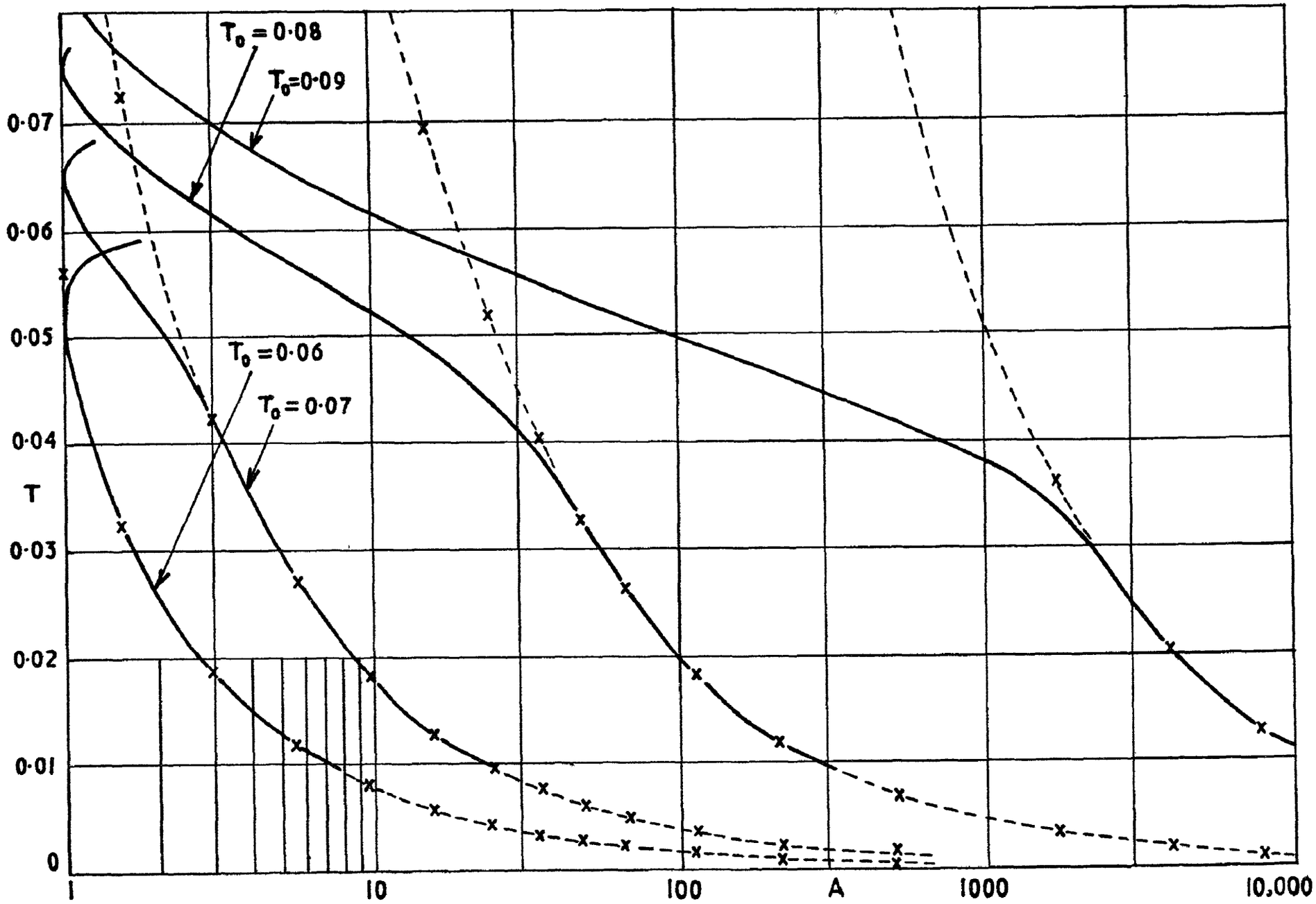

Equilibrium – Isentropic flow $p_0 = 10^{-7}$

FIG. 11.

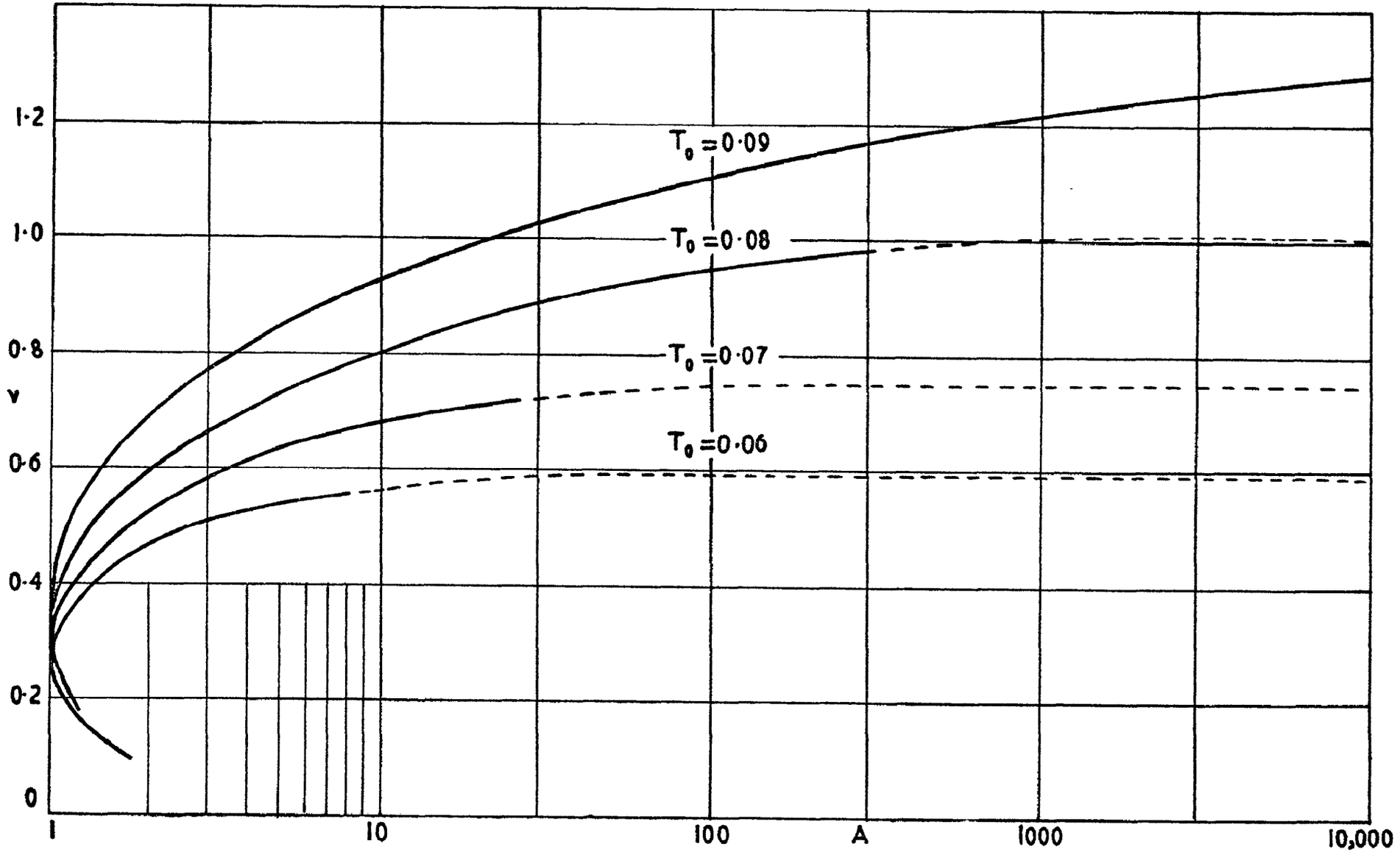

Equilibrium – Isentropic flow $p_0 = 10^{-7}$

FIG. 12.

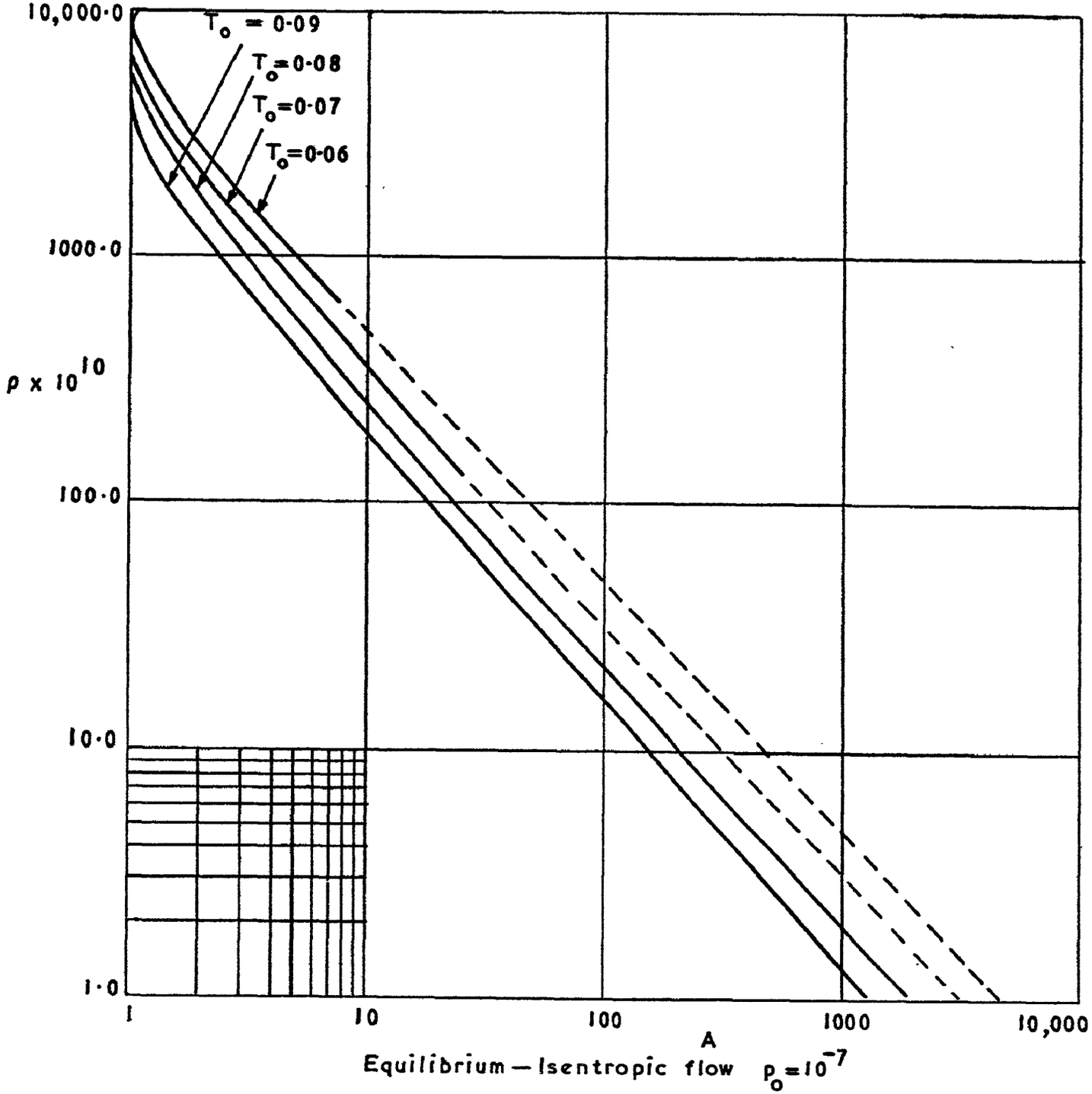
10,000·0
1000·0
100·0
10·0
1·0
ρ x 10^10
T_o = 0·09
T_o = 0·08
T_o = 0·07
T_o = 0·06
1
10
100
1000
10,000
A
Equilibrium — Isentropic flow p_o = 10^-7

FIG. 13

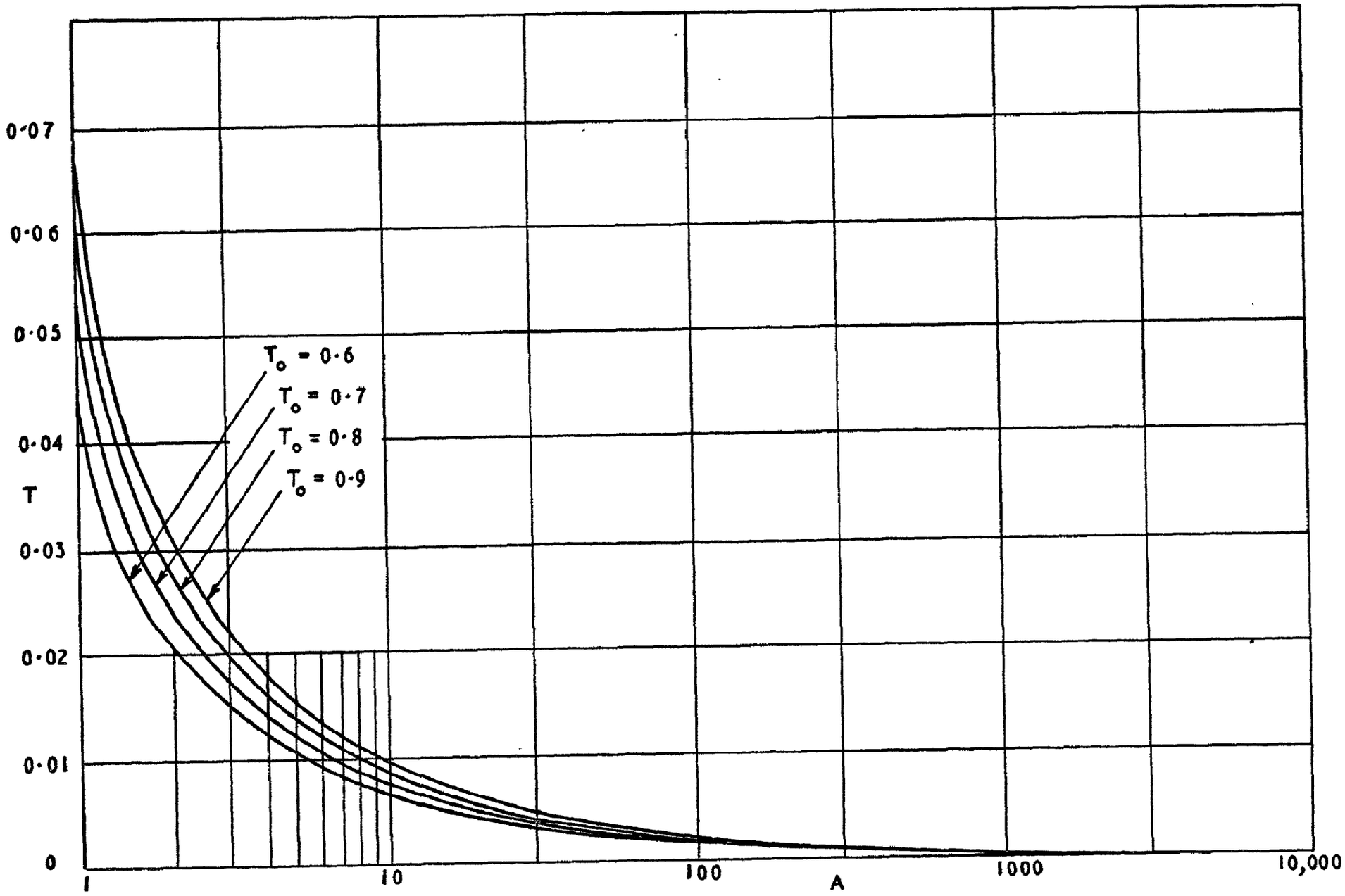

FIG. 14

Frozen – Isentropic flow – All pressures

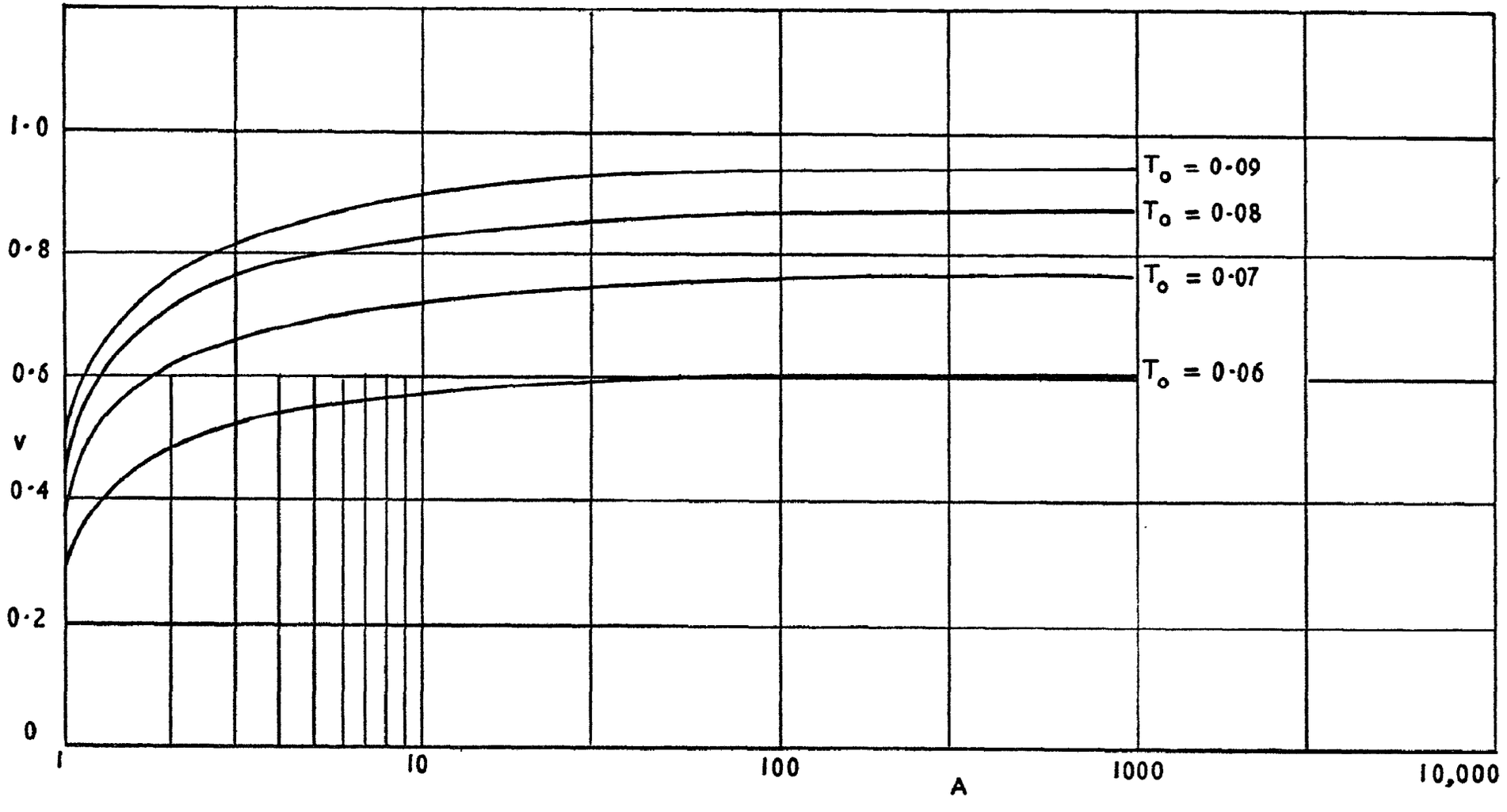

Frozen — Isentropic flow $p_o = 10^{-9}$

FIG. 15

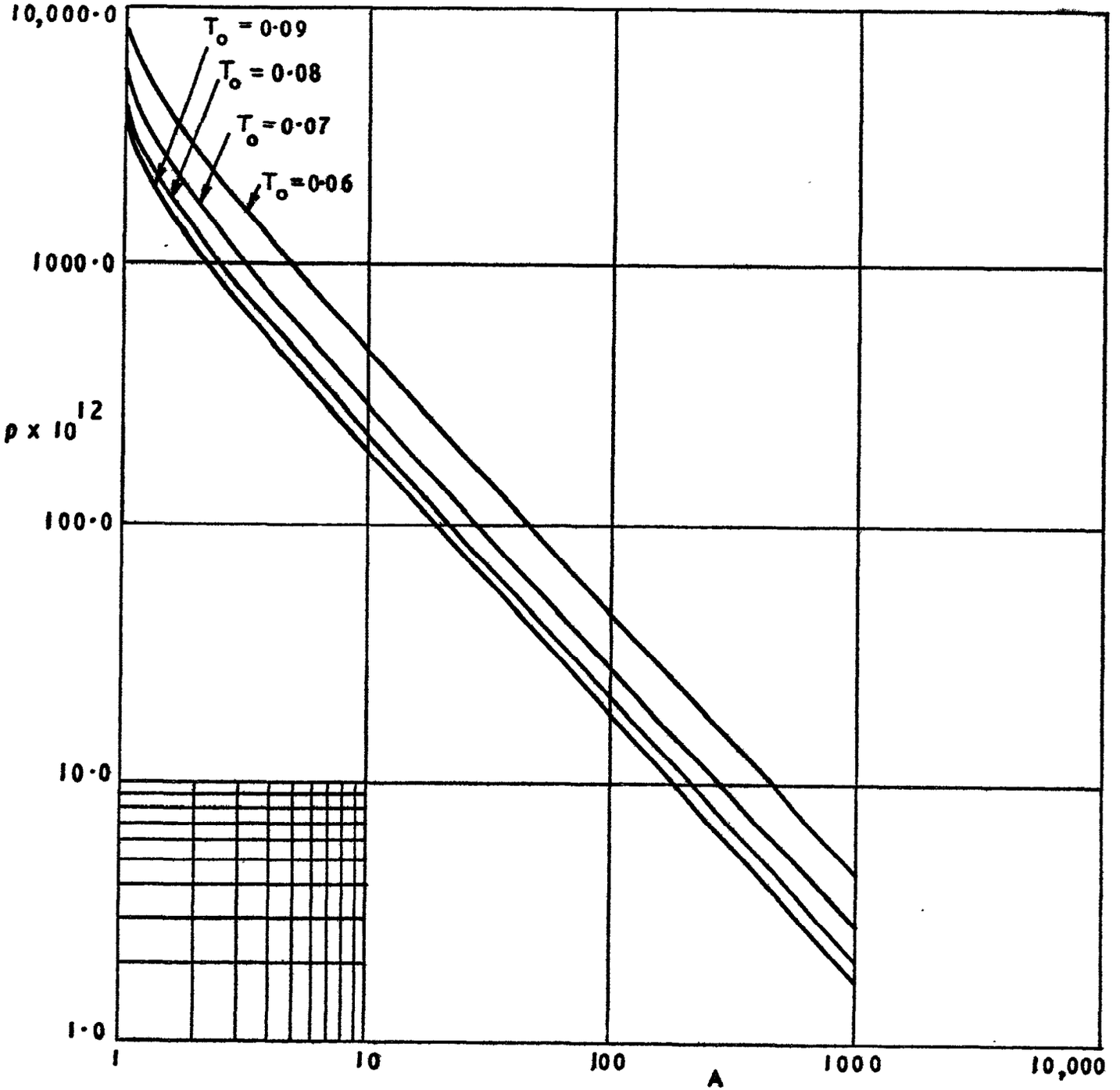
10,000·0
1000·0
100·0
10·0
1·0
ρ x 10^12
T_o = 0·09
T_o = 0·08
T_o = 0·07
T_o = 0·06
1
10
100
1000
10,000
A

FIG. 16

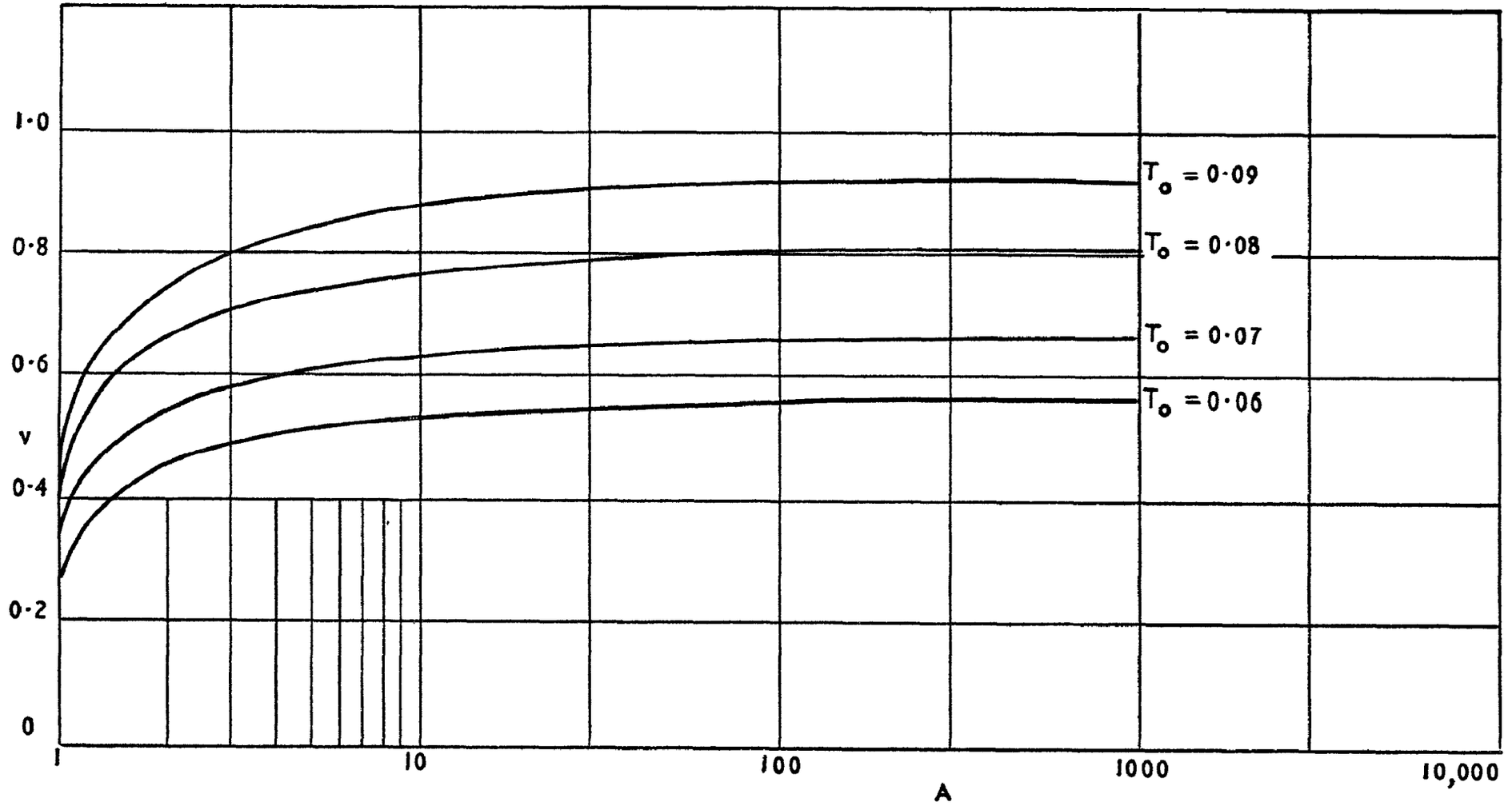

Frozen - Isentropic flow $p_o = 10^{-8}$

FIG. 17

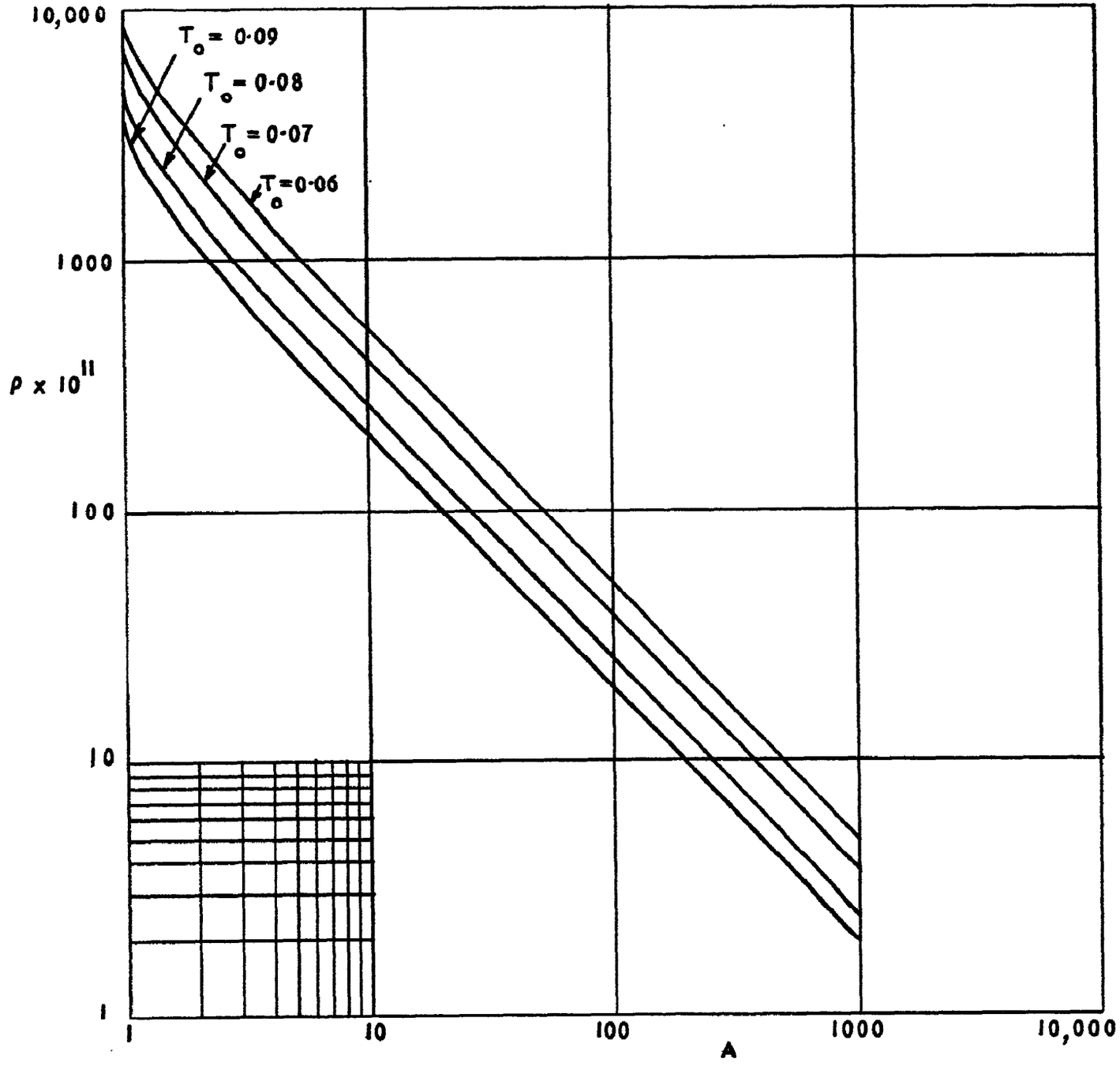
10,000
1000
100
10
1
ρ x 10^11
T_o = 0·09
T_o = 0·08
T_o = 0·07
T_o = 0·06
1
10
100
1000
10,000
A

FIG. 18

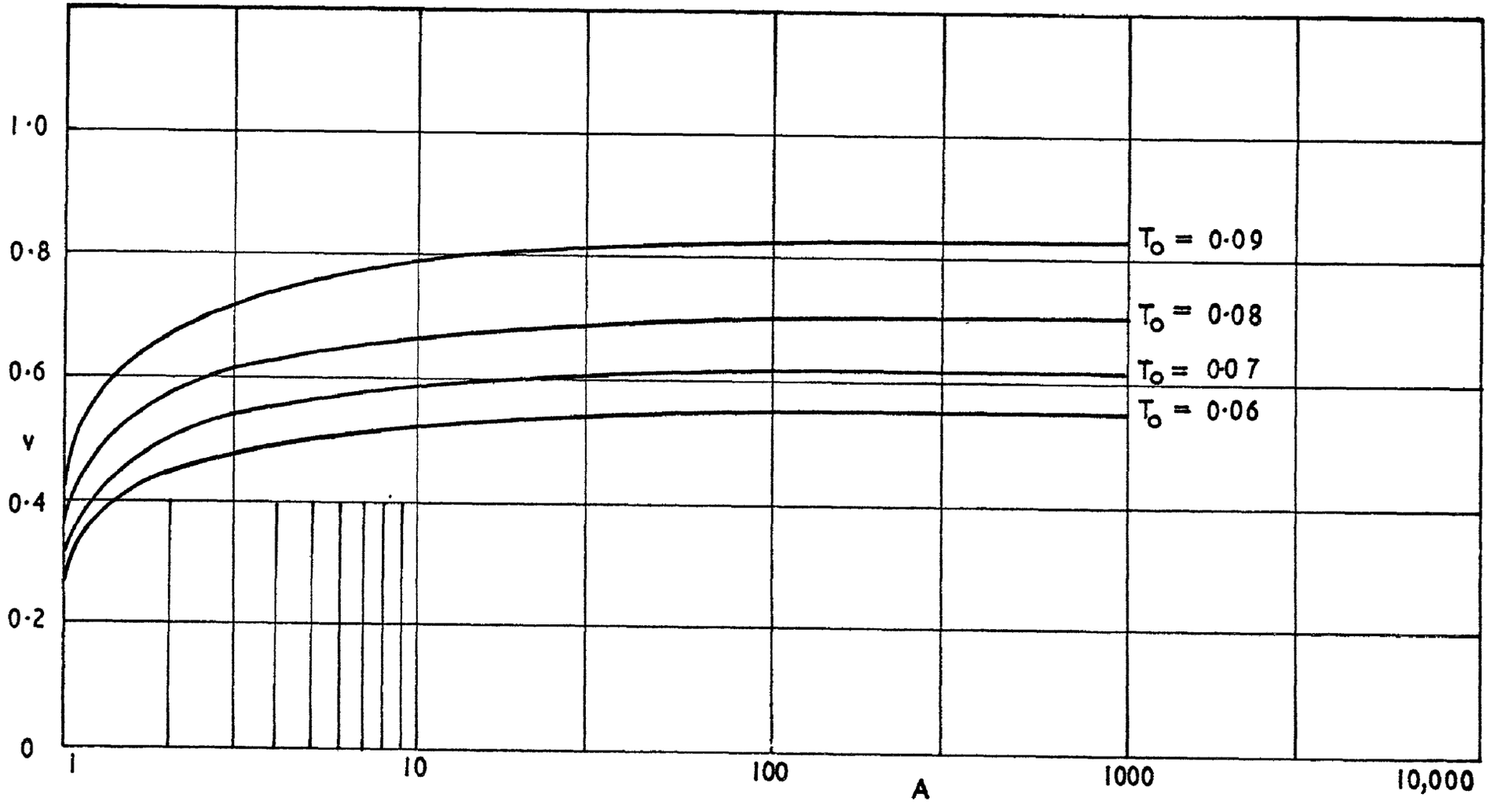

FIG. 19.

Frozen-Isentropic flow $p_o = 10^{-7}$

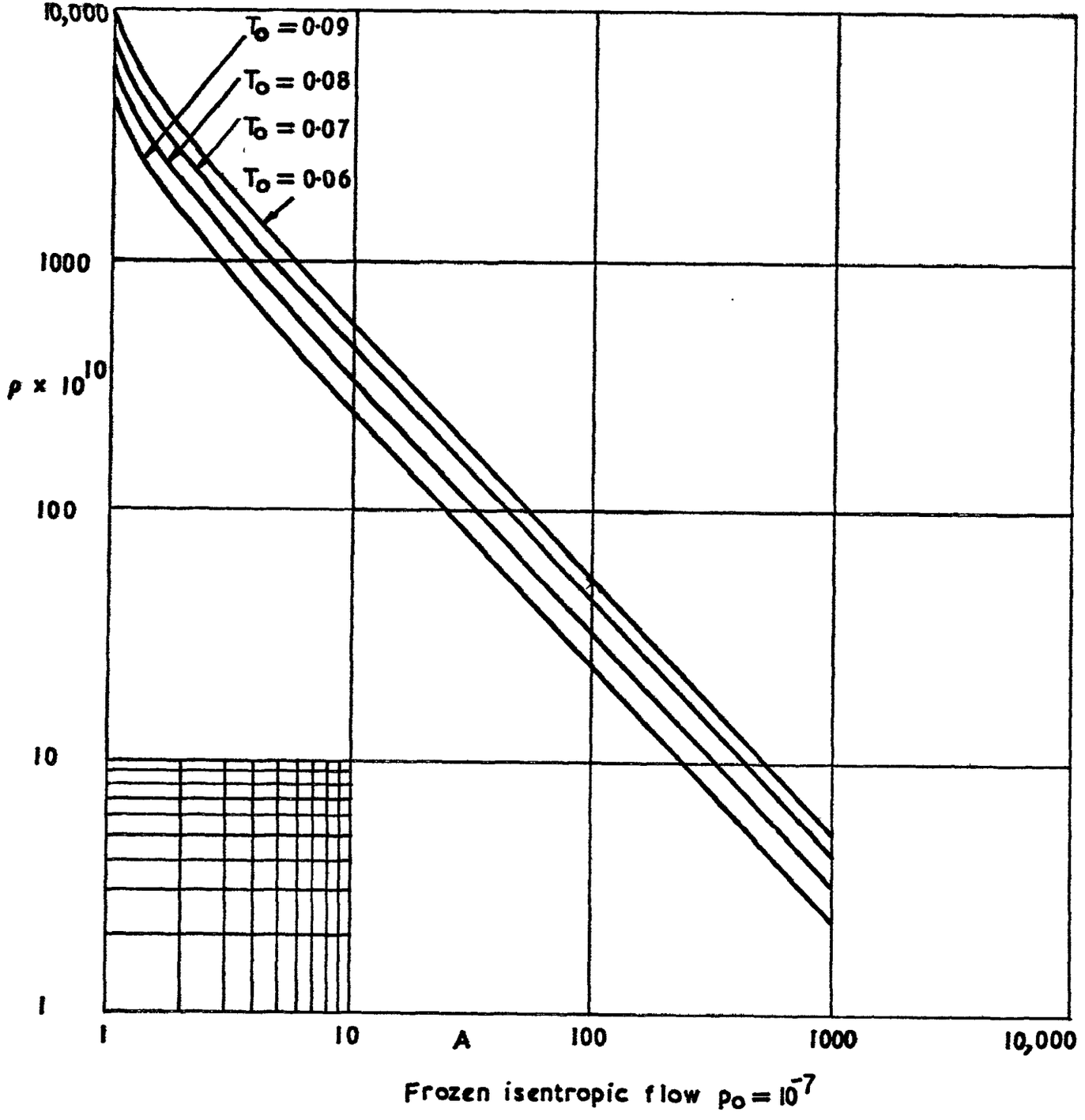
10,000
1000
100
10
1
$\rho \times 10^{10}$
$T_o = 0{\cdot}09$
$T_o = 0{\cdot}08$
$T_o = 0{\cdot}07$
$T_o = 0{\cdot}06$
1
10
A
100
1000
10,000
Frozen isentropic flow $p_o = 10^{-7}$

FIG. 20.

FIG. 21

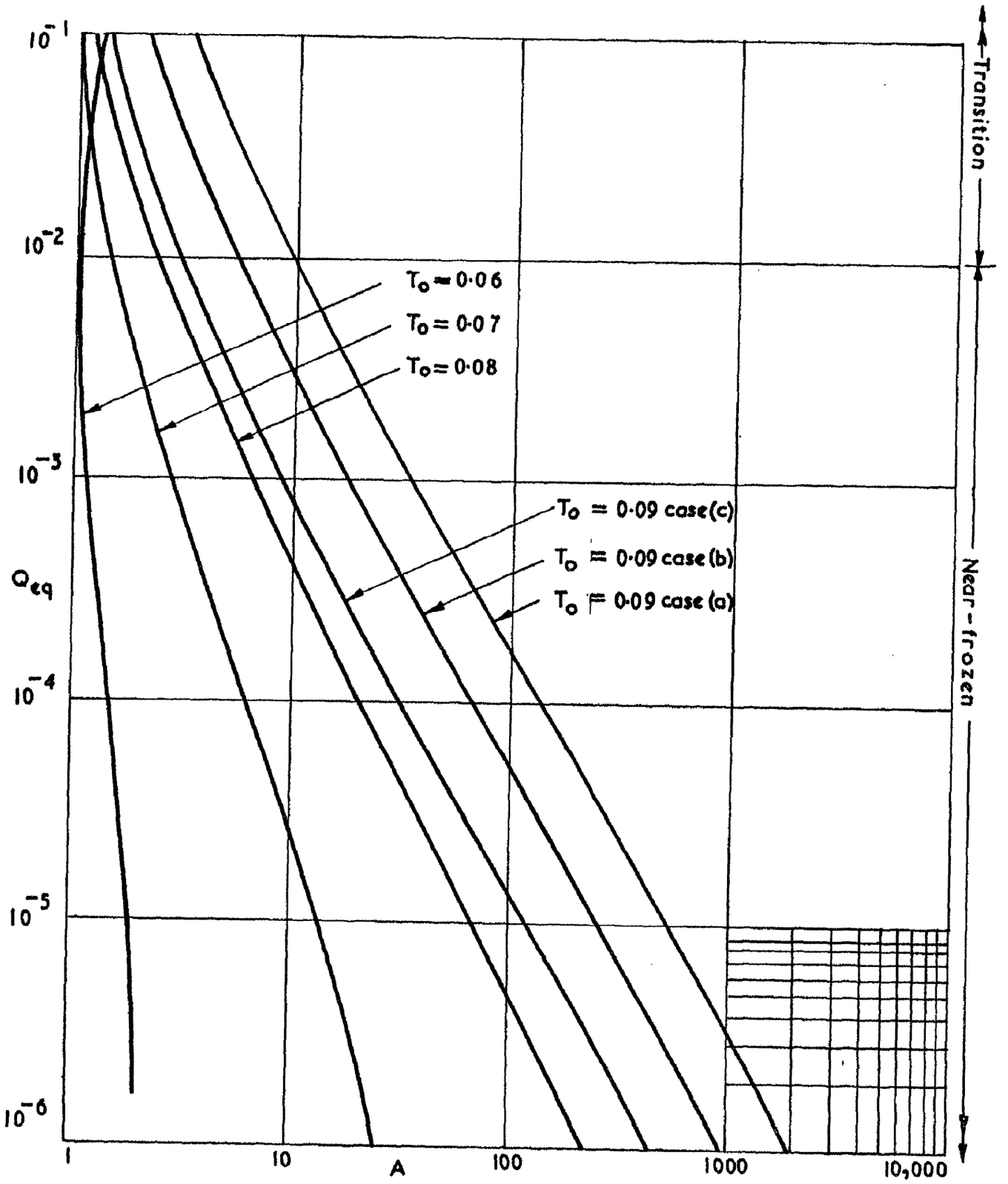

Test for equilibrium flow $p_o = 10^{-8}$

FIG. 22.

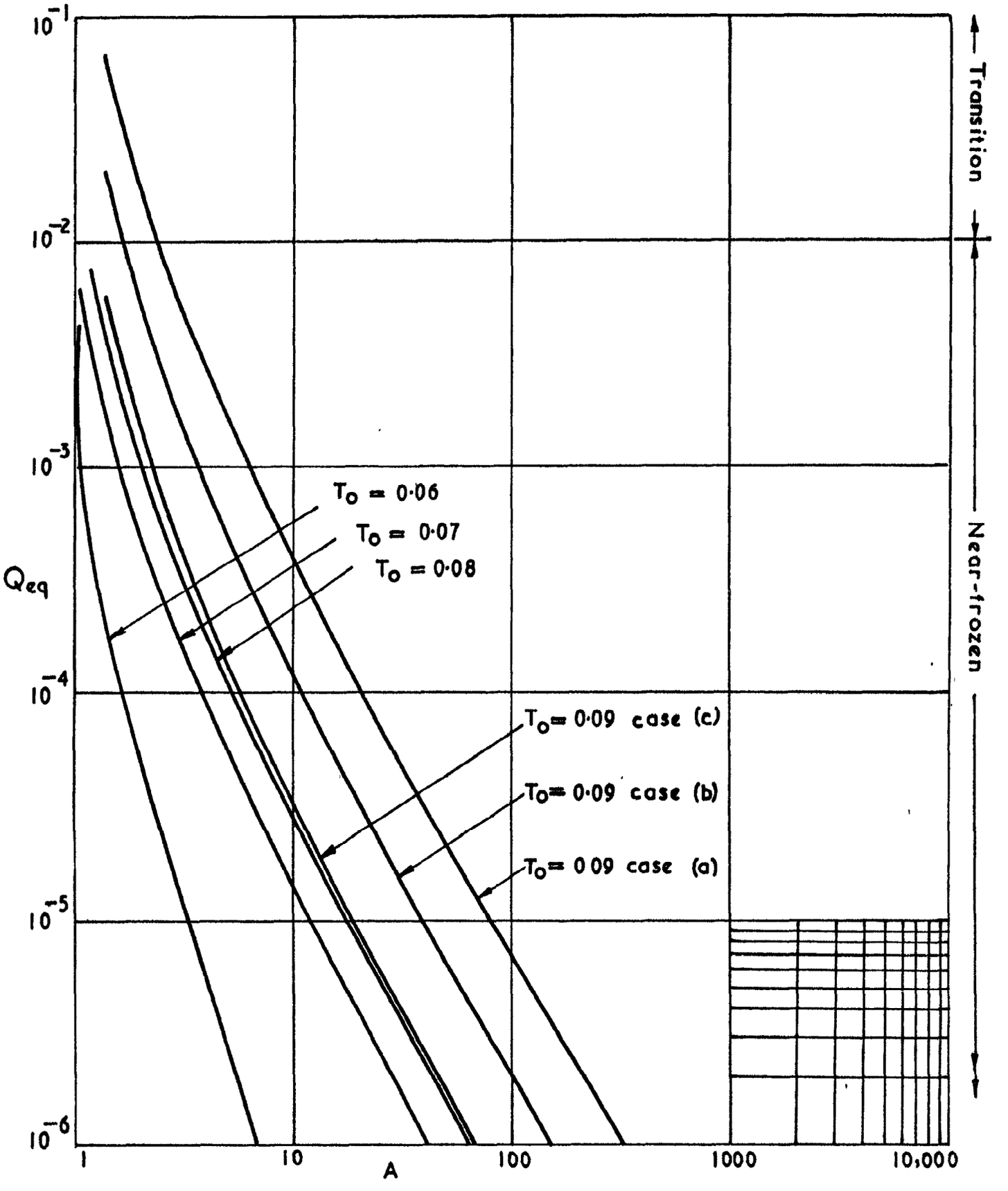

Test for equilibrium flow $p_o = 10^{-9}$

DS97056/1 WHB1 K4 10/61 XL

Printed and published by
HER MAJESTY'S STATIONERY OFFICE

To be purchased from
York House, Kingsway, London W.C.2
423 Oxford Street, London W.1
13A Castle Street, Edinburgh 2
109 St. Mary Street, Cardiff
39 King Street, Manchester 2
50 Fairfax Street, Bristol 1
2 Edmund Street, Birmingham 3
80 Chichester Street, Belfast 1
or through any bookseller

Printed in England

S.O. Code No. 23-9012-59